

Digital process planning of joining by numerical models in the automotive industry

OSCAR ANDERSSON

Doctoral Thesis No. 9, 2017
KTH Royal Institute of Technology
Industrial Engineering and Management
Department of Production Engineering
SE-100 44 Stockholm, Sweden

TRITA-IIP-17-09
ISSN 1650-1888
ISBN 978-91-7729-536-5

Akademisk avhandling som med tillstånd av KTH i Stockholm framlägges till offentlig granskning för avläggande av teknisk doktorsexamen fredagen den 15 december kl. 10:00 i sal M311, KTH, Brinellvägen 68, Stockholm.

Abstract

The automotive industry is striving towards reduction of greenhouse gas emission by reducing product weight and improving fuel efficiency of their products. The introduction of lightweight materials have imposed greater pressure not only on the product development but also on manufacturing systems. One integral aspect of manufacturing systems, which is meeting these challenges is joining technology. In order to achieve successful joining of new automotive products, joining process planning must be equally successful.

This research aims at improving process planning of joining by introducing digital tools into the process planning work method. The digital tools are designed to reduce lead times and increase accuracy of the process planning to realize more advanced, complex and environmentally friendly product solutions in the vehicles of the future.

The research has two main focuses. Firstly, the joining process planning structure and organization have been analysed. The analysis has identified specific instances where digital tools can be introduced to improve the process planning and make it more efficient. Digital tools, such as numerical models for prediction and databases for re-use of knowledge, have been suggested for the process planning. An assessment of the impact of the introduction of these tools in an industrial test case has been performed to show the possible reduction in lead times.

Secondly, geometrical distortions due to laser beam welding have been investigated, both by experimental trials and numerical modelling. The influences of design and process parameters on the distribution and magnitude of geometrical distortions have been established. Numerical models of different modelling detail and complexity have been developed and evaluated in order to find modelling approaches with reduced computation times aimed at industrial implementation. The predictive accuracy and computational efficiency of the numerical models have been assessed and evaluated with regard to industrial implementation.

Sammanfattning

Fordonsindustrin strävar efter minskade utsläpp av växthusgaser genom lättare produkter och produkternas förbättrade bränsleeffektivitet. Införande av lättviktsmaterial har ökat utmaningarna för såväl produktutveckling som produktionssystem. En central del av dessa produktionssystem, som påverkas av utmaningarna är fogningsteknik. För att uppnå fullgod fogning av nya produkter i fordonsindustrin krävs även fullgod processplaneringen av fogningsprocesser.

Denna forskning syftar till att förbättra processplanering av fogningsprocesser genom att införa digitala verktyg i arbetsmetodiken för processplanering. De digitala verktygen är utvecklade för att minska ledtider och öka processplaneringens noggrannheten för att förverkliga mer avancerade, komplexa och mer miljövänliga produktlösningar i framtidens fordon.

Forskningen har två huvudfokus. För det första har processplaneringen av fogningsprocesser analyserats. Analysen identifierade specifika punkter där digitala verktyg kan användas för att förbättra processplanering och öka dess effektivitet. Digitala verktyg, t.ex. numeriska modeller för prediktering och databaser för återanvändande av kunskap har föreslagits för processplaneringen. En bedömning av inverkan av användningen av de digitala verktygen har gjorts för att visa den möjliga minskningen i ledtid.

För det andra har geometriska distorsioner på grund av lasersvetsning undersökts genom såväl experimentella försök och numerisk modellering. Konstruktionens och processparametrars inverkan på utbredningen och magnituden av de geometriska distorsionerna har fastställts. Numeriska modeller med olika nivåer av detaljrikedom i modelleringen och komplexitet har utvecklats och utvärderats för att hitta modelleringsätt med minskade beräkningstider ämnade för industriell implementering. Den prediktiva noggrannheten och beräkningseffektiviteten av de numeriska modellerna har bedömts och utvärderats med avseende på industriell implementering.

Acknowledgement

First and foremost, I would like to express my sincere gratitude to my supervisor Professor Arne Melander for his guidance and immense knowledge during the research process. I am also very grateful for his patience, encouragement and motivation during the final stages of the completion of this thesis.

I would like to thank Karl Fahlström at Swerea KIMAB for companionship and interesting discussions about the research and cooperation during the experiments.

In addition, I would like to thank my colleagues at Volvo Car Corporation, Urban Todal, Niclas Palmquist, Gert Larsson, Martin Olsson, Magnus Arvidsson and Lars-Ola Larsson who have all helped me with their knowledge and interesting discussions during the research. Also, I would like to thank Glen Hopkins and Esa Laurila for their help in the laser lab.

Also I would like to thank my family and friends for their invaluable encouragement during the research.

Finally, a very special thank you is due to Emma, who supported me and showed understanding during the late evenings and weekends when I completed this thesis.

List of appended papers

Paper A

O. Andersson, D. Semere, A. Melander, M. Arvidsson, and B. Lindberg, "Digitalization of Process Planning of Spot Welding in Body-in-white," in *Procedia CIRP*, 2016, vol. 50

Paper B

O. Andersson, N. Budak, A. Melander, and N. Palmquist, "Experimental measurements and numerical simulations of distortions of overlap laser-welded thin sheet steel beam structures," *Welding in the World*, vol. 61, no. 5, 2017

Paper C

O. Andersson, A. Melander, and K. Fahlström, "Experiments and efficient simulations of distortions of laser beam welded thin sheet closed beam steel structures", Accepted for publication in *Journal of Engineering Manufacture*, 2017

Paper D

O. Andersson, A. Melander, and K. Fahlström, "Verification and evaluation of simulation methods of laser beam welding of thin sheet steel structures", Submitted for publication in *Journal of Material Processing Technology*, 2017

Contents

1	Introduction.....	1
1.1	Scope of thesis.....	3
1.2	Research questions and hypotheses.....	3
1.3	Research methodology.....	5
1.4	Introduction to the papers.....	6
1.5	Contribution of the present author to the papers.....	8
1.6	Relation to licentiate thesis of the research.....	9
1.7	Outline to the thesis.....	10
2	Theoretical framework	11
2.1	Process planning of joining processes.....	11
2.2	Laser beam welding principles.....	14
2.3	Geometrical distortions due to welding.....	17
2.4	Numerical modeling of the laser beam welding process.....	20
3	Methods.....	25
3.1	Joining process planning.....	25
3.2	Material selection.....	26
3.3	Experimental set-up.....	27
3.4	Welding equipment and process parameters.....	30
3.5	Experimental result evaluation and analysis.....	30
3.6	Numerical modeling of laser beam welding.....	31
4	Results and discussion.....	33
4.1	Digital process planning of joining.....	33
4.2	Geometrical distortions due to laser beam welding.....	37

4.3	Numerical modeling of geometrical distortions due to laser beam welding.....	44
5	Conclusions and future research	56
5.1	Conclusions	57
5.2	Future research.....	58
	References	60
	Appendix A	64

1 Introduction

During the recent decades, producers and consumers have been required through legislation to reduce greenhouse gas emissions to reduce the effects of global warming [1]. Moreover, these requirements are expected to increase in the future [2]. The automotive industry is presently one of the dominant sources of greenhouse emissions [3] due to extensive fuel emissions caused by their products. The automotive industry's response to these requirements has thus far been reducing fuel consumption by producing more fuel efficient or alternative fuel engines [4] and reducing the weight of their products [5].

The reduction in weight of vehicles is done by innovative design concepts and use of materials of high strength to weight ratios in the body in white. Such materials include high-strength steels, aluminium and composite materials [6]. Figure 1 shows the material composition, including high content of ultra high strength steels of Volvo Car Corporation's XC90 body in white structure introduced in 2014. These solutions are associated with challenges due to their material properties and novelty and complexity of the associated manufacturing processes [7].

One of these challenging manufacturing processes is joining, which is an integral part of modern automotive manufacturing. In the conquest for lighter products, joining technology is in constant development to be able to produce light products with high quality, high repeatability and robustness and complex designs [8].

In order to achieve products and manufacturing systems with such properties, process planning and pre-engineering work is essential. Traditionally, process planning has been performed by physical experimental work in laboratory environments to optimize and confirm manufacturing systems. Such physical based process planning is dependent on material supply and equipment availability may require prolonged lead times and material waste. One way of reducing the lead

times for the process planning is by digital methods such as numerical simulations. In addition, a digital process planning approach may reduce waste, increase product quality and make more optimal designs possible.

One measure of product quality is geometrical accuracy, which is critical to achieve sufficient product strength and is one of the aspects of the process planning. As joining in manufacturing will affect product geometry, geometrical distortions is a critical challenge for joining engineers in industry. Furthermore, it is a challenge with increasing significance as thinner and lighter materials with more slender designs are introduced.

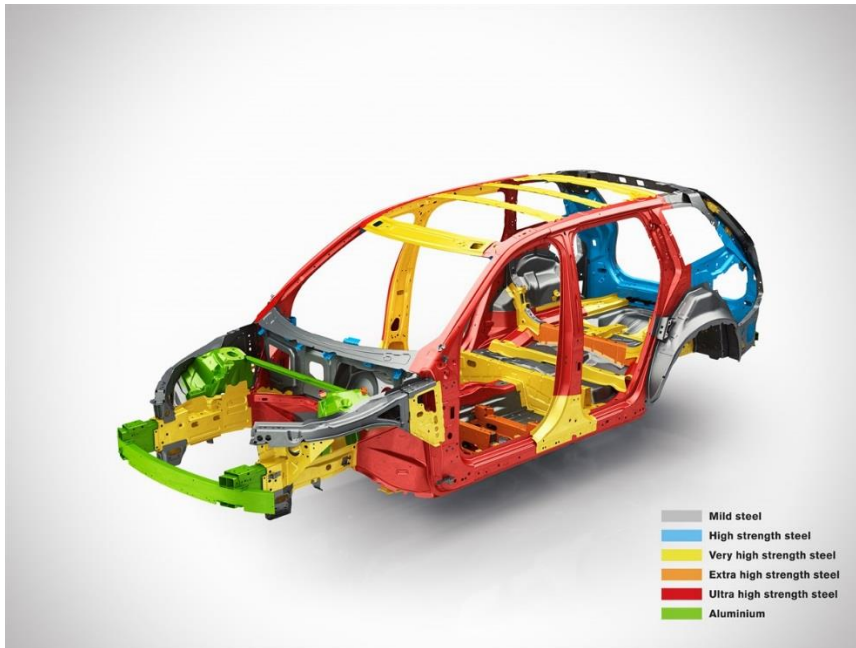


Figure 1 Material composition of the body in white of Volvo Car Corporations XC90. [9]

Moreover, in order to achieve high strength products with lower weight, high strength joints are required. Therefore, continuous joints by, for example laser beam welding (LBW) or adhesives, are an advantageous alternative compared to traditional discrete joints, such as resistance spot welding (RSW) or self-piercing rivets (SPR). However, continuous joints may also increase material disturbances during manufacturing, which may increase geometrical distortions.

In the present thesis, a digital process planning approach is described and showcased for RSW, the most dominant joining method for automotive steel structures, and compared to a traditional physical process planning approach. The description highlights the advantages of digital engineering and the possible reduction in lead times of using digital process planning work.

As a part of the digital process planning approach, the thesis includes an investigation of numerical predictions of geometrical distortions due to LBW. The investigation presents influencing factors determining geometrical distortions and methods to predict and analyse geometrical distortions due to LBW in light-weight structures in a time and computation efficient manner.

From the two parts above, a digital process planning approach is developed both in terms of work flow, organisational structure and numerical modelling contents, for implementation in industry.

1.1 Scope of thesis

The aim of this thesis is to present a digital process planning approach for joining processes, which reduces lead times and is less wasteful of materials without renouncing accuracy compared to traditional physical process planning. The digital process planning approach is composed of two sub-parts. Firstly, an organizational and work flow part, which describes the structure of digital process planning. Secondly, a part which includes a numerical modeling approach to predict geometrical distortions due to LBW.

An additional aim is to increase understanding of the thermal and mechanical behavior of steel structure during welding in order to increase accuracy of modeling of the LBW process. By increasing the understanding of the thermal and mechanical behavior, the numerical models can be made more efficient in terms of time and computation power required by implementing relevant and accurate simplifications in the models.

1.2 Research questions and hypotheses

The present thesis aims to answer four research questions, which treat different aspects of digital process planning of joining. By answering the research questions an improved understanding of digital process planning

can be established leading to better industrial solutions, with shorter lead times and higher accuracy in production.

The first question regards the capabilities of a digital process planning method of joining engineering.

- **I: Can process planning of joining processes be carried out with digital engineering tools?**

The second question regards significant factors of the LBW process and is stated as follows.

- **II: What process and materials factors affect the magnitude and distribution of geometrical distortions due to laser beam welding?**

The third question regards numerical modelling of the LBW process.

- **III: How accurately can numerical models predict geometrical distortions due to laser beam welding?**

Finally, a fourth question regards efficiency of numerical modelling of the LBW process.

- **IV: What simplifications can be done to numerical models while maintaining sufficient accuracy of results?**

The four research questions above form the scope of the research in the thesis. As basis for the research questions the following research hypotheses have been developed, respectively.

- **I: Digital engineering tools can be utilized to carry out process planning of joining processes.**
- **II: Heat input, mechanical and thermal material parameters and global structural shape all affect the distribution and magnitude of geometrical distortions due to laser beam welding.**
- **III: Numerical models can predict geometrical distortions with sufficient accuracy to be beneficial to process planning.**

- **IV: Material models, heat transfer models, and numerical modeling can be simplified to become more efficient with maintained accuracy for engineering applications in industry.**

1.3 Research methodology

To be able to answer the research questions and prove or disprove the research hypotheses a rigorous research framework has been used as methodology. The theoretical background for the framework is obtained from research done in several fields, ranging from statistics, geometrical distortions, material science, material modelling and numerical modelling methods. Scientific papers, journals and books have been studied to create the theoretical base of the thesis. The results of the thesis are taken from case studies, physical experiments and numerical modelling.

The digital process planning approach was developed from previous research results applied to case studies taken from industry and extended by innovative process planning. The process planning approach was developed in close collaboration with industrial partners to assure industrial relevance and enabling industrial implementation.

The experimental work on distortions of LBW was carried out in a semi-industrial environment to assure the industrial relevance of the research while keeping the accuracy of academic research. The materials used in the research are of industrial relevance ranging from mild steels to ultra-high strength steels (UHSS), all used in modern automotive components for different applications. Furthermore, the analysis of the experimental work was carried out with several different methods such as macroscopic measurement of geometrical distortions and microscopy analysis of cross-sections of the weld zones.

The numerical modelling was performed on several different software and hardware configurations, ranging from simplified models with general numerical modelling software to specialized numerical modelling software with specific features developed to predict geometrical distortions due to heat. By using several different software, the research can both evaluate the accuracy of the numerical predictions as well as evaluate the potential for industrial implementation.

1.4 Introduction to the papers

Appended are four papers, which compose the research of the thesis. The papers treat several aspects of process planning including the general framework a digital process planning approach and the details of the numerical methods of the LBW process. Together, they form the results to answer the research questions above. Each of the papers is briefly introduced below and described how they answer the research questions introduced earlier.

1.4.1 **PAPER A: Digitalization of process planning of spot welding in body-in-white**

Published in *Proceedings 26th CIRP Design Conference*, 2016

Paper A analyses the process planning flow in modern automotive production with regard to resistance spot welding. It describes the traditional way of working which is based on physical tests to set parameters for welding. These parameters are essential to produce high quality welds which do not create additional interruptions or need for reparation in production due to weld spatter. As this physical process is costly and time consuming due to material deliveries and dependence on specific equipment a digital process planning method, with shorter lead times and less dependence of equipment, could be more beneficial. The paper describes the work flow and identifies critical instances where digital alternatives could be as advantageous as possible. The paper also present digital alternatives in terms of numerical models and makes an attempt to establish the benefit in terms of lead time for an entire car project. This attempt highlights the potential for digital process planning and works as a promising background for the following research in papers B, C and D.

1.4.2 **PAPER B: Distortions of overlap laser welded thin sheet steel beam structures**

Published in *Welding in the World*, 2017.

Paper B investigates geometrical distortions due to LBW of mild steel beam structures, both through experiments and numerical simulations. The study includes two basic geometrical shapes, 1000 mm in length, which resembles beam like automotive body in white components. The study proposes significant factors which affect the distribution and magnitude of the geometrical distortions. These factors are heat input, bending stiffness, distance between the rotational centre and the laser weld line. By

identifying these factors, design guidelines are proposed which can be used to reduce geometrical distortions both by structural design and process planning. In tandem, a for-industry developed simplified software solution was evaluated. The software solution's accuracy was evaluated and its drawbacks were highlighted. The accuracy was deemed helpful for industry in several of the test cases as it could predict basic distortion mode and indicate the magnitude of distortions in several of the cases. However, for the more extreme cases where non-linear or non-continuous physical effects took place, the simplified model could not capture the experiments accurately. Possible improvement factors and limitations of the study were also identified and work as groundwork for the following papers.

1.4.3 **PAPER C: Experiments and efficient simulations of distortions of laser beam welded thin sheet close beam steel structures**

Accepted for publication in *Journal of Engineering Manufacture*, 2017.

Paper C complements the study in Paper B by extending the experimental and numerical study by including higher strength materials, namely DP600 and a press hardened boron alloyed 22MnB5 steel. Both these materials are extensively used in automotive body in white production in applications where high strength is essential, such as structural pillars or transverse or longitudinal beams. The material extension increases the industrial relevance of the research. Moreover, the geometry of the steel beams were changed to 700 mm compared to paper B. In this paper, the basic parameters which affect the distortions were confirmed for the new specimens. In addition the numerical simulations were performed with a general numerical modelling software, which increases the potential for industrial implementation as this kind of software is readily available and more widespread compared to the software used in paper B. Furthermore, the general software enabled more customisation and modelling freedom, which resulted in two different modelling approaches with different level of modelling detail. These two modelling approaches were compared in terms of accuracy and efficiency.

1.4.4 **PAPER D: Verification and evaluation of simulation methods of laser beam welding of thin sheet steel structures**

Submitted for publication to *Journal of Material Processing Technology*, 2017.

Paper D works as a continuation of the study in Paper C. In this paper the numerical models are complemented with a third model with additionally increased level of detail. In this final numerical model, several non-linear and non-continuous physical phenomena are modeled. Naturally this increases the modeling complexity and thereby computational time of the simulations. Paper D works as a benchmarking between different numerical modeling approaches and their benefits and limitations for a digital process planning approach. The conclusion of Paper D is that the most detailed model achieves the highest accuracy and agreement to the experiments while it consumes significantly more computational power and time compared to the other more simplified models. A discussion is carried out regarding the use of the different levels of models in industry.

1.5 Contribution of the present author to the papers

1.5.1 Paper A

Andersson defined the hypothesis of the research, defined the virtual process planning approach and evaluated the virtual work flows. Andersson also contributed with the industrial application and insight to the research. Semere contributed with the definition of the physical and virtual work flows. Melander contributed with scientific discussions and suggestions to the manuscript.

1.5.2 Paper B

Andersson defined the hypothesis of the research, planned the experiments, designed the experimental set-up, conducted the welding experiments and carried out experimental raw data gathering and experimental result analysis. Andersson also developed the numerical model and carried out numerical simulations and wrote the scientific paper. Budak and Palmquist contributed to the experimental welding and scientific discussions. Melander contributed with scientific discussions and suggestions to the manuscript.

1.5.3 Papers C and D

Andersson defined the hypothesis of the research, planned the experiments, designed the experimental set-up, conducted the welding experiments and carried out experimental raw data gathering and experimental result analysis. Andersson also developed the numerical model and carried out numerical simulations, wrote the scientific paper. Fahlström contributed to the experimental welding, experimental result gathering and analysis and scientific discussions. Melander contributed with scientific discussions and suggestions to the manuscript.

1.6 Relation to licentiate thesis of the research

The licentiate thesis “Process planning of resistance spot welding”, defended in 2013, by the present author works has a close relation to the present doctoral thesis as it has similarities in both its research questions and its theoretical topics. The licentiate thesis developed and evaluated numerical modeling principles for resistance spot welding by accuracy and agreement to physical experiments.

The licentiate thesis showed promising results by general good agreement between numerical simulations and experiments. The present thesis is a continuation and works as an extension by including the results from the licentiate thesis to a more comprehensive digital process planning approach, which also includes organizational aspects as well as implementing the results to an industrial context. The present thesis is also a complement to the licentiate thesis by including numerical modeling of a second joining method, i.e. LBW.

The papers included in the licentiate thesis are listed below.

- O. Andersson and A. Melander, “Statistical Analysis of variations of resistance spot weld nugget sizes,” in *IIW International Conference on Global Trends in Joining, Cutting and Surfacing Technology*, Chennai, India 2011, 2011, pp. 870–875.
- O. Andersson and A. Melander, “*Statistical Analysis of Variations in Resistance Spot Weld Results in Laboratory and Production Environment*,” The 5th Swedish Production Symposium, Linköping, Sweden, 2012.
- O. Andersson and A. Melander, “*General regression models for prediction of spot weld sizes*,” in International congress on advances in welding science and technology for construction energy and transportation systems, IIW Congress, 2011, Istanbul, Turkey, 2011.
- O. Andersson and A. Melander, “*Verification of the capability of resistance spot welding simulation*”, AWS Sheet Metal Welding Conference XV, Livonia, USA, 2012.
- O. Andersson and A. Melander, “*Prediction and verification of resistance spot welding results of ultra high strength steels through FE simulations*,” Modeling and Numerical Simulation of Material Science. 2015;5:26-37.

1.7 Outline to the thesis

There are in total five chapters in the present thesis. Following this introductory chapter, a presentation of the theoretical background of the subjects is made in Chapter 2. The background chapter includes a description of typical process planning work for joining processes including activities, actors, requirements and a timeline. The theoretical background also includes a description of the physical phenomena behind the LBW process, background about geometrical distortions due to joining and theoretical background regarding numerical modelling approaches of the LBW process.

The background chapter is followed by Chapter 3 describing the methods used in the research. The chapter includes methods regarding the development of the digital process planning approach as well as details and reasoning behind the regime of the LBW physical experiments.

The methods chapter is followed by a summary of the results gained from the appended papers in Chapter 4. The results include the proposed digital process planning approach including both organisational structure taken and possible gain. The result chapter also includes results of the physical experiments and numerical modelling of geometrical distortions due to LBW. The results are evaluated in terms of agreement between experiments and models and in terms of computational efficiency.

Lastly, the thesis includes a chapter with the conclusions of the thesis and answers to the research questions in Chapter 5. A discussion regarding the results and possible future research in the field is also included in the final chapter.

2 Theoretical framework

In the following chapter the theoretical framework related to the research is presented. The theoretical framework forms the basis of the research and is relevant to the new results presented later in the thesis. This chapter presents basic principles related to the process planning of joining processes and theories specific to the numerical modeling of the LBW process.

2.1 Process planning of joining processes

Process planning of joining processes aims to assure sufficient results of a given process before larger scale industrial production is implemented. Process planning is essential due to the uncertainties and partially unmonitored processes in large scale industrial production, such as in the automotive industry. In order to assure the results of the joining in

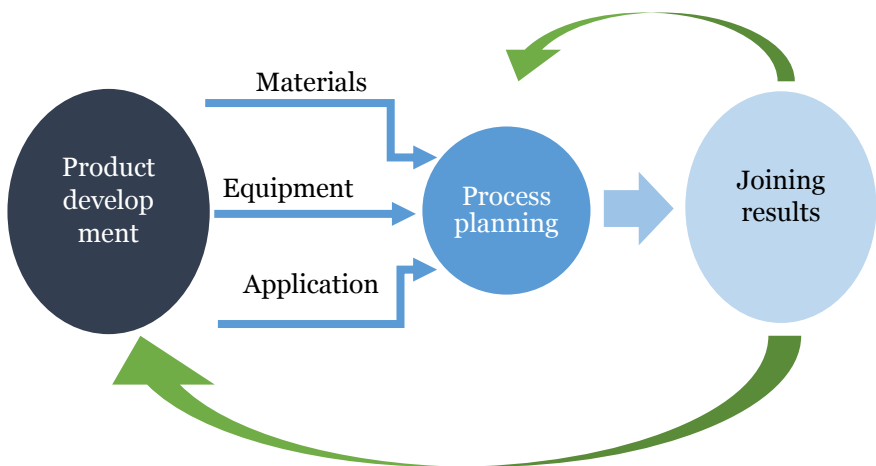


Figure 2 Typical iterative work flow of process planning of joining processes

production, small scale experiments are carried out and evaluated in controlled lab environments and often with geometrically simplified and generalized specimens. The results of the process planning may be used to update and improve the product design or the manufacturing process as illustrated in Figure 2.

This traditional physically based approach to process planning has been used in industry for many decades. However, as will be illustrated in the present thesis, process planning may instead be based on digital tools to assure results of joining processes. According to the hypothesis of the present theses, a digital process planning approach may be able to reduce lead times and costs compared to the physical process planning, which is of increased interest in the present industrial landscape.

To evaluate a joining process' results, several multiple different criteria can be defined which represent the outcome of a industrialized manufacturing process. As the present thesis treat the two joining methods RSW and LBW, Table 1 lists the most relevant aspects of evaluation for process planning of the two joining processes. Traditional experimental process planning includes established experimental setups to test these evaluation criteria. Table 1 also forms a comprehensive list of demands and requirements on the capabilities of digital tools for process planning, which shall replace the established experiments to form a digital process planning approach. While all of the listed evaluation criteria are relevant to all joining processes to some degree, the table represents a prioritized list of criteria based on process planning experiences from industry and its most common challenges [10], [11].

Table 1 Evalutaion criteria for process planning of joining processes

Evaluation criteria	Unit of evaluation	LBW	RSW
Local weld size	mm	X	X
Global geometrical distortions after welding	mm	X	
Surface quality of weld	-	X	X
Cracks in weld	-	X	
Porosity or voids inside weld	%	X	
Weld expulsion during welding	-		X
Location accuracy of weld	-	X	

As the Table illustrates, the two joining process both share evaluation criteria and have criteria which are unique to the process. To include all the prioritized criteria in the table in the thesis is out of the scope of the present research. The thesis will focus on the geometrical aspects of the weld results, i.e. the weld size and the distortions due to welding. To investigate these criteria is a relevant initial update of process planning for industry.

In process planning several entities can be identified, which both act as submitters of requirements of the joining process and receivers of results of the joining process planning. These entities are normally associated with specific departments within engineering firms in industry. Examples of these entities are styling designers, design engineers, manufacturing engineers, industrial technicians and end consumers [12]. All these players put demands on the joining process or its results, which are critical to the feasibility of the joining process. These demands are captured in the evaluation criteria mentioned above.

The results from the process planning often works as a feedback to a possible re-design or re-development of the product or the process. In that way, the process planning is an iterative part of a design loop where product development and manufacturing systems have to compromise to reach a final solution industrial solution. As the iterative nature of the process between product development and manufacturing systems may be unavoidable due to the complexity of the investigations and as each iteration adds lead times to the product realisation time, the possible gain with a digital process planning approach is enhanced for each iteration.

As a comparison, during the past decades several aspects of the product development process have been greatly enhanced and increased in efficiency by digital tools and computer aided design (CAE) tools such as the Finite Element Method (FEM) or Computational Fluid Dynamics (CFD). These tools are used to predict and optimize product properties such as stiffness, weight, durability, aerodynamics, etc and are today the primary tool for many aspects of the product development pre-engineering work [13].

In order to make to entire product realization process more time efficient all steps must make use of digital tools. Digital tools and CAE solutions have in the previous decades indeed been developed to model joining processes in order to predict joining results and to evaluate the above named criteria for RSW and LBW [14]. However, due to the complexity, multi-physical nature and non-linearity of the physical phenomena of

joining processes [14], which require extensive computational power and competence (often exclusive to research environments) as well as considerable natural variations in actual joining results, the industrial use of these digital tools are still limited or reserved to specific investigations without wide spread general implementation.

The present trend is that computational power is becoming more powerful and cost efficient to industry and digital tools have become more user-friendly. Moreover, the requirement for reduced lead times is ever increasing. Thus, as implied by the first research hypothesis of the thesis, the outlook for the future is that digital tools for joining process planning are on the rise.

As second aspect to the digitalization of joining process planning, in addition to the predictive abilities of the digital tools described above, is the efficient storage and re-use of existing knowledge from previous joining results and investigations. By implementing and maintaining a database with previous results future investigations that can be accessed efficiently, the lead times can be reduced even more.

2.2 Laser beam welding principles

As mentioned above, LBW is a common joining method in many industries including automotive and naval industries. The main advantages of LBW are the high strength continuous joints with low material impact, high geometrical accuracy and high surface quality of the final weld. In the following chapter the main basic principles of the LBW process, its process parameters and their impact on the final joining results are described.

Laser is an abbreviation of Light Amplification by the Stimulation Emission of Radiation. As the name suggests, a laser is a construction which amplifies light (increases in power) by a mechanism known as *stimulation emission*. In its most basic form a laser is constructed of two reflecting mirrors with an active medium between them, which causes the stimulated emission. Many types of active media can be used, in solid, liquid or gas form. The mirrors and active medium are collectively known as a *cavity*. In industrial lasers, one of the mirrors is partially transparent in order to let a laser beam emerge. [10]

The amplification of light is based on the quantum mechanical phenomenon stimulated emission, first theoretically described in 1916 [15] and later observed in 1928. When the atoms of the active medium are stimulated external energy, they may release excess energy in the form of

additional light. The electrons of the atoms of the active medium absorb energy and gain an energy level through excitation (by light) and they generally become unstable. The supply of energy to the active medium is known as pumping and is generally done by electrical current. The unstable condition of the electrons causes the electrons to drop energy level again and release the excess energy as additional light. Thus, the light becomes amplified. This mechanism is repeated due to the reflective mirrors inside the cavity and the pumping of the active medium. [16]

Above, the basic principles of laser technology are described. In LBW applications a laser beam is generated (usually in the order of 10^4 W mm^{-2}) and aimed at a metal work piece to generate enough heat to melt and join the materials by solidification. The laser beam produces a thin but deep vapour cavity, known as a *keyhole*, in the material. The keyhole is created by the vaporization which creates multiple reflections inside the cavity. The keyhole remains in equilibrium between forces due to vapour pressure and forces due to molten material outside the keyhole.

In LBW the work piece material absorbs energy by two main mechanisms: *inverse bremsstrahlung* absorption (also referred to as *plasma absorption*) and *Fresnel absorption*. The inverse bremsstrahlung is the transfer of energy from photons to electrons and is the main absorption mechanism at higher heat input levels. Fresnel absorption takes place at the multiple reflections inside the keyhole and is dominant at lower heat input levels [17].

The laser source itself and the application in LBW can be altered in numerous ways. These alterations are controlled either by the laser equipment or through user controlled process parameters. The most important process parameters are covered in the following chapter.

The **laser source** can be made of several different source materials including gases, e.g. CO_2 , solid state materials, e.g. Nd:YAG or fibre based materials or fibre disk materials. The laser source material will affect the beam quality, the material absorption, the energy efficiency and the possible power output of the laser equipment. In LBW, the dominant source was earlier CO_2 lasers but due to the limitations in power output, the trend in LBW is towards other solid state laser sources.

The **welding power** of the laser beam is of great importance to the weld result. Insufficient welding causes power lack of penetration while excessive welding power may cause dropout welds or geometrical distortions. These limits are dependent of material, sheet thickness and

welding speed. In many cases in industry the welding power is set close to the upper limit in order allow for process variations with maintained results [17]. Another aspect of welding power is the delivery mode; both a continuous wave and pulsed waves can be used. Pulsed waves can be used when heat input should be minimized in order to avoid certain weld defects such as cracking or porosity. However continuous waves are better from an efficiency perspective [17].

The **welding velocity** is, like welding power, a measure of the heat input and will result in lack of penetration or dropout welds if not optimized. In addition, a few other aspects of welding speed are relevant [10]. With varying welding velocity the molten weld pool pattern and size changes. Lower speeds increases the width of the weld pool and the risk of dropout increases. Higher welding speeds, on the other hand, increases the risk of the weld pool to not have enough time to redistribute to form a joint and may form an undercut weld instead [17].

A general outline of the relation between welding velocity and welding power and their resulting weld shapes are shown in Figure 3. The cross section weld shapes themselves are illustrated in Figure 4.

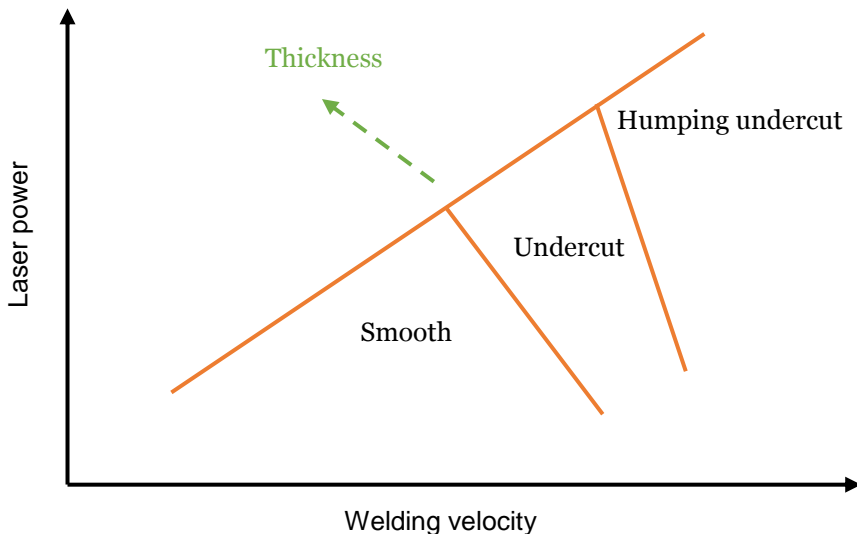


Figure 3 Schematic relation between welding power and welding speed and associated weld results. Adapted from [10]

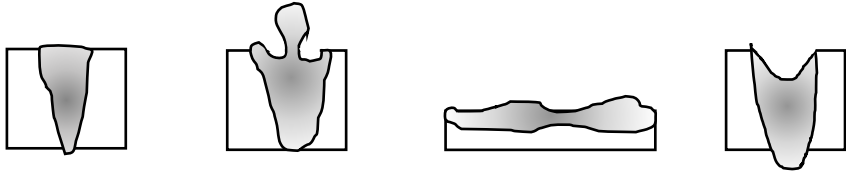


Figure 4 Weld shapes connected to welding velocity a) normal/good b) undercut c) humping d) dropout. Adapted from [10]

The **focal point's** location relative to the sheet surface has effect on the penetration depth of the weld. Studies have shown that depending on beam diameter and focal length, the optimum focus point is approximately 1 mm below the sheet surface. The reason for the focus depth is that the heat generation should be optimized to generate and maintain a keyhole inside the work piece for maximum penetration. A lower - or deeper - focus point will result in less weld penetration. [10]

In LBW, **process gases** may have three functions; shielding the molten weld pool from the atmosphere, suppression of the plasma and protection of the laser optics. The shielding of the weld pool (from both the top and bottom side of the work piece) may be necessary to prevent weld defects by oxidation and contamination. Secondly, at high welding powers and low welding speeds plasma formation is higher and the excess plasma will defocus the beam and reduce the heat energy absorption of the weld. The result may be an undercut weld, see Figure 4. By using a gas jet the plasma can be removed from the critical zone and avoid such plasma effects. Thirdly, weld spatter may damage surrounding equipment in the working environment. A gas jet can direct the weld spatter in a certain direction and avoid such damages [17]. When welding thin sheet materials, as studied in the present thesis, the effect of shielding gases are quite low and normally only compressed air is used during welding [17].

2.3 Geometrical distortions due to welding

In welding a heat source moves along the weldment, resulting in drastic local rise in temperature. The temperature increase will induce thermal strains in the structure and cause microstructural changes to the welded material. Sequentially, as the heat source is removed, the temperature will fall and solidification of the weldment takes place. During the cooling and solidification the atoms in the crystal lattice will re-arrange and assume their fixed positions. All of the above-mentioned phenomena – thermal strains, microstructural changes and re-arrangement of atoms – will cause dimensional changes to the structure which will cause global geometrical

distortions of the welded structure. In addition to the basic phenomena of the material's behavior during its temperature cycle during welding, the mechanical and thermal boundary conditions and restraints of the structure will affect the magnitude and distribution of the global geometrical distortions.

The heating of the material causes volumetric expansion in and near the weld and is controlled by the coefficient of thermal expansion. However, during the expansion the welded material isn't free to move and stresses will form. By considering an idealized cross-section of a welded plate, illustrated in Figure 4, the causes and mechanisms during welding can be discussed. When the welded material is heated and expands the surrounding material is restraining the expansion resulting in compressive stresses further away from the weld centre. In the following step when the zone near the weld is cooling and tries to contract, the surrounding metal is restraining the contraction. While the Figure shows a transverse cross-section, the above reasoning is true in all directions surrounding the weld.

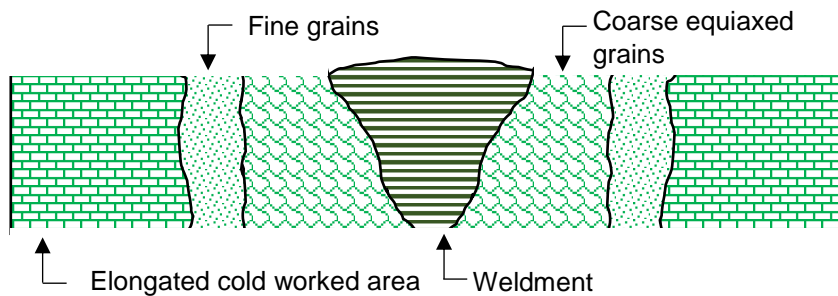


Figure 5 Idealized cross-section of a welded plate

The dominant mode or modes of distortion in a certain application or structure is dependent on several factors, including joint type, welding process and structure geometry. In Figure 6 the basic modes of geometrical distortions due to welding are illustrated. In the present research, LBW of overlap joints in thin sheet steel materials in tubular structures are studied. In such a configuration, transverse shrinkage, longitudinal shrinkage and longitudinal bending are the dominant distortions modes and will be discussed in more detail.

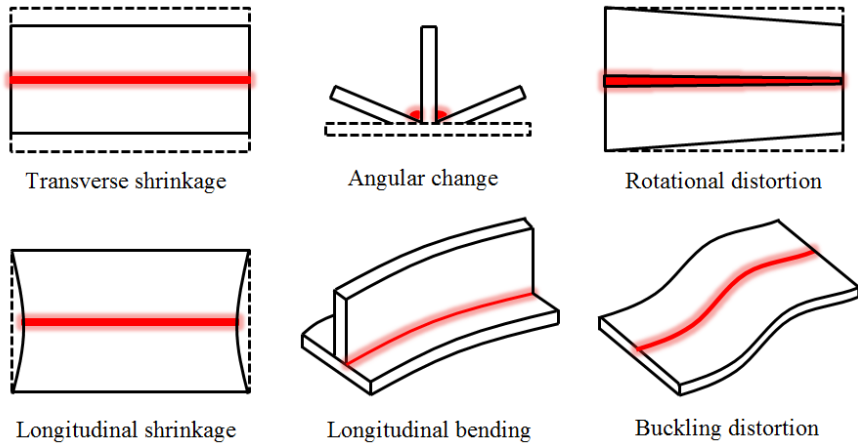


Figure 6 Basic geometrical distortions modes due to welding

Transverse shrinkage is controlled by the heating and cooling of the cross-section as explained above. The magnitude of the shrinkage is dependent on the distribution of the elevated temperature zone as well as the mechanical properties of the welded material, the degree of restraint of the structure and the plate thickness.

The longitudinal shrinkage is similar to the transverse shrinkage, however, the temperature potential between higher and lower temperatures is created at different points along the weld path. Thus, it is a continuous phenomenon where the tensile and compressive regions are moving along the weld path during the welding sequence. In addition, the forces caused by the longitudinal strains will create a bending moment if the weld path is not co-existing with the neutral plane of the structure. When the bending moment is exerted to the structure, longitudinal bending deformations occur. The magnitude of the longitudinal shrinkage and bending deformations are dependent of the heat input of the weld source as well as the mechanical properties of the welded material and the structural restraint of the welded structure, i.e. bending stiffness.

As geometrical accuracy is of high importance to the industry in order to achieve high product quality and avoid post-welding repair or material scrapings, geometrical distortions due to welding are important to mitigate. Several attempts and several methods have been proposed to minimize welding distortions including optimization of process parameters [18] and welding sequence [19], control by clamping and fixturing [20], [21], [22], [23], control by thermal tensioning [24], [25],

mechanical tensioning [26] and pre-welding geometrical compensation [27]. In addition, a field of research has focused on modeling of the welding process to simulate welding distortions, in order to optimize the welding process further, as will be explained in the remainder of this chapter.

2.4 Numerical modeling of the laser beam welding process

As described above, the LBW process includes multiple physical phenomena, several which are dependent of each other. In order to numerically model the LBW process and the geometrical distortions due to it, these phenomena must be included in the model. Several modeling approaches have been proposed during the last decades ranging from highly detailed local models of the keyhole based on both FEM and CFD solutions to more simplified and time efficient models based on FEM or historically even more simplified models.

Generally, the modeling involves a thermal part of the model, which computes the temperature field of the structure and a mechanical field, which translates the temperature field to strains and deformations in the structure. These two parts, and possible simplifications, are treated separately below.

2.4.1 Thermal modelling

The thermal model of LBW is based on a constitutive model controlled by a set of thermal loads and boundary conditions. The constitutive model is the general transient heat problem, as given in Equation 1 below.

$$k \left[\frac{\partial^2 T}{\partial x^2} + \frac{\partial^2 T}{\partial y^2} + \frac{\partial^2 T}{\partial z^2} \right] + \dot{Q} = \rho C_p \frac{\partial T}{\partial t} \quad (1)$$

In Equation 1 k is the thermal conductivity, T is the temperature, Q is the internal heat generation, ρ is the density and C_p is the specific heat and t, x, y, z are the time and spacial coordinates, respectively.

A critical part of LBW modelling is the modelling of the heat source, Q in Equation 1. One of the earliest models of welding heat sources in general was published by Rosenthal [28] and was based on a point heat source. The model was later further developed by Swift-Hook and Gick [29] as a line heat source through the material thickness moving relative to an infinite material in the sheet direction. The model was further developed by Steen et al [30], who combined the point and line sources to model the shape of a LBW keyhole. Another proposed model is a surface heat source of

Gaussian distribution as developed in two papers by Lax [31], [32], which may be more appropriate for convection mode LBW, where less penetration of the heat in the thickness direction takes place.

In welding modelling in general, most commonly arc based welding methods, a 3-dimensional double ellipsoid model proposed by Goldak [33] in the 1980s is the most used. The model assumes a Gaussian distribution of heat input over the double ellipsoid volume. It has been proved accurate for arc based welding modelling, however for deep penetration methods such as LBW or electron beam welding it has been shown less efficient.

In the 1980s a 3-dimensional double ellipsoid model was proposed for numerical modelling, such as Finite Element modelling, of the welding process and is still commonly used [25]. It is used to model both shallow penetration welding methods such as arc welding and to lesser extent deep penetration welding methods such as LBW or electron beam welding. The heat input is distributed as a Gaussian function over the ellipsoid volume.

An alternative conical Gaussian model for LBW has also been proposed [34]. It can be described as a moving line source model. The line heat source at any given time is defined according to Equation 2.

$$q(r, z) = \frac{2Q}{\pi r_0 H} \exp\left(1 - \left(\frac{r}{r_0}\right)^2\right) \left(1 - \frac{z}{H}\right) \quad (2)$$

In Equation 2, Q is the laser beam power, r_0 is the initial radius of the keyhole and H is the depth.

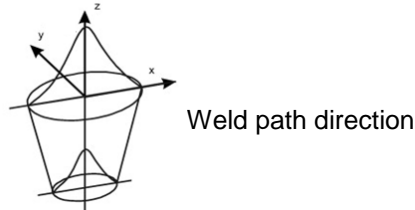


Figure 7 Moving conical Gaussian heat source model. Adapted from [35]

As can be seen in Equation 2 and Figure 7 the conical Gaussian model assumes reduced power intensity in the thickness direction. However, in thin sheet applications, where full penetration welds may be desirable, the reduction of heat intensity over the thickness is lower. Therefore, some research [36] has neglected the variation of heat generation in the thickness direction in the model. Mathematically, it can be expressed by removing the final term of Equation 2, resulting in Equation 3.

$$q(r) = \frac{2Q}{\pi r_0 H} \exp\left(1 - \left(\frac{r}{r_0}\right)^2\right) \quad (3)$$

While the above-mentioned models have been used for macroscopic numerical modelling of structural problems, they only treat the heat conduction between the material and the laser beam. The actual physical phenomena in keyhole welding, however, include multiple additional physical mechanisms besides heat conduction. Some efforts have been made to fully model the physics of the keyhole.

Several keyhole models are based on energy and/or pressure balance between the walls of the keyhole. Kroos et al [37] assumed a cylindrical keyhole through the sheet thickness, which was concentric to the laser beam. The model could describe the stability of the keyhole. Kaplan et al [38] proposed a model, which relied on the energy balance between the keyhole walls at numerous points through the thickness and could thus calculate the keyhole size and the laser weld profile in a cross section. Lankalapalli et al [39] assumed a conical keyhole shape and developed a model which could calculate penetration depth. A further development was made by Fabbro and Chouf [40], which included the fluid flow inside the keyhole. It treated the back and front walls of the keyhole separately and could thus also find the size of the keyhole. Often the more detailed keyhole models are not implemented in full-scale FE models but evaluated for the keyhole itself.

On the other hand, the transient conduction models have often been shown to be too computer power demanding to perform efficient simulations of global structures. Therefore, efforts have been made to reduce the complexity of the thermal modelling to increase efficiency of the simulations by means of modelling simplicity based on several assumptions.

One often used assumption is that cooling contraction is the dominant source of distortions, as early proposed by Okerblom [41]. The so-called shrinkage model was proposed to predict distortions based on this assumption [42]. The shrinkage model applies an instant reduction of temperature in the region near the weld during one computation step, modelling the cooling contraction. The reduction of temperature is equal to the temperature difference from the solidification temperature to ambient temperature. The model was used for both simple idealized geometries [43] and more complex geometries [44] albeit with post-welding calibration.

2.4.2 Mechanical and metallurgical modelling

The mechanical model for LBW can be summarized by Equation 4, showing the strain components of the model.

$$\varepsilon = \varepsilon_E + \varepsilon_p + \varepsilon_{th} + \varepsilon_m \quad (4)$$

In Equation 4 the right hand side components represent elastic strain, plastic strain, thermal strain and metallurgical strain respectively.

The elastic strain is modelled by Hooke's law through Young's modulus and Poisson's ratio. At stresses above the yield stress, plastic deformations take place and are controlled by a defined flow stress curves. The thermal strains are controlled by the thermal expansion coefficient and the temperature field taken from the thermal model. The metallurgical strains are due to phase transformations in the material and take place during heating or cooling during the temperature cycle.

Both the elastic and plastic strains are highly temperature dependent. The Young's modulus and the yield stress are both drastically reduced with elevated temperatures, see Figure 8.

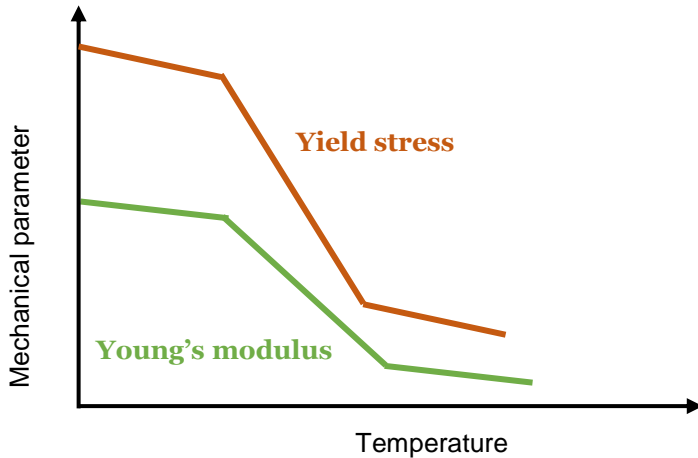


Figure 8 Idealized behaviour of mechanical parameters at elevated temperatures

Furthermore, the thermal strains, controlled by the coefficient of thermal expansion, is near linear at a wide range of temperatures but exhibits non-linear behaviour at temperatures associated with austenitization during

heating and martensitic transformation during rapid cooling, see a schematic representation in Figure 9. Finally, the metallurgical strains due to martensitic transformation is highly complex and rarely included in models other than for welding specific FEM software.

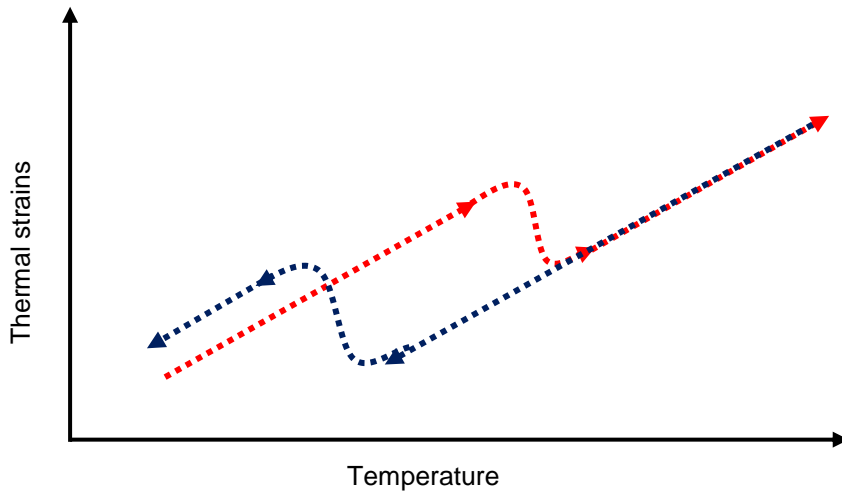


Figure 9 Idealized behaviour of thermal strain during heating (red) and martensitic cooling (blue)

In summary, the mechanical model of the LBW process is highly complex and in order to include all physical phenomena a high amount of input data is required. However, to ascertain all modelling data is time consuming and expensive, in particular high temperature physical material testing. Thus, it is of interest to investigate the possibility to reduce the complexity of the material model in order to reduce computation times and to reduce the need for material input data for simulations.

3 Methods

This chapter aims to describe the research methods used in the thesis. The chapter treats the method of analysis of the process planning, as well as the material selection, the set-up and equipment, the welding process parameters and evaluation methods of the experimental regime. The numerical modeling approach of these methods are treated in Chapter 4.3

3.1 Joining process planning

In order to propose an improved approach to joining process planning by implementing digital tools, a present joining process planning way of working was analysed thoroughly by value stream mapping. In the research, a case study at the automotive OEM Volvo Car Corporation's (VCC) body in white departments was conducted.

In the case study the process planning of RSW process parameters was analysed. The process planning aims to find process parameters to assure product quality in terms of joint strength and assure manufacturing robustness by avoiding weld spatter. The case study was examined in terms of interviews with key actors in the product development and manufacturing engineering departments at VCC. Moreover, the author was involved in work in the manufacturing engineering department at VCC during the research, which allowed an insight into the way of working at the company.

The analysis considered three aspects of the joining process planning; the functional, temporal and logical aspects. The functional aspect analysed the roles and iterative loops of exchange of information, data and tools during the process planning. The temporal aspect identified the time required to perform the process planning in order to find critical aspects to reduce lead times. The logical aspect analysed the requirements and demands of the process planning and what conditions that must be fulfilled to trigger certain activities.

The aim of the test case was to determine the structure and organisation of the joining process planning by analysing through the three above-mentioned aspects. Furthermore, it aimed to identify and estimate the experimental work and the digital tools used in the process planning. By this determination, identification and estimation, typical lead times of the present process planning can be assessed. It can also be used to identify relevant points where digital tools can be used to reduce the lead times.

The digitalized process planning approach was developed based on digital tools which have been developed and evaluated by the author in previous research. The present research aims to evaluate the possible reduction in lead times by implementing the digital tools into an industrial test case. The analysis of the present process planning approach combined with the results of the digital process planning tools are used to determine a possible reduction of lead times if they were implement into the process planning.

3.2 Material selection

The sheet materials in the present research are all materials commonly used in the automotive industry for LBW applications. Thus, thin sheet steel materials with a thickness of 1.0 mm and 1.5 mm of varying strength were chosen. Lower grade steel materials with an approximate yield strength of 200 MPa and higher strength UHSS material with yield strengths above 1000 MPa were investigated as well as intermediate conventional high strength dual phase steels. In automotive applications, the lower strength materials are often used for outer panels such as roofs, doors or tailgates due to their beneficial formability. The stronger UHSS material are often used for structural load bearing components such as floor beams or pillar components due to their high strength and high crashworthiness. In both these applications LBW is a common joining method and to minimize geometrical distortions due to welding is of importance both for geometrical assurance and structural integrity.

The nominal values for alloying contents are presented in Appendix A and the mechanical properties are presented in Table 2. The 22MnB5 material had an AlSi coating formed during the hot forming process in its production. The other materials were uncoated, i.e. without any corrosion protection Zn coating. While most sheets in automotive applications are Zn coated it is also associated with a lower robustness in LBW due to higher risk of weld spatter and porosity in the weldment. As geometrical distortions is the focus of the present research and it is assumed that the

Zn coating has little effect on the distortional behavior of the specimens, uncoated materials were selected for the study.

Table 2 Nominal tensile strength of steel materials

	Tensile strength
VDA-100 CR-3	200 MPa
Mild steel	200 MPa
DP800	800 MPa
22MnB5	1500 MPa

3.3 Experimental set-up

The materials of the research – as described above – were formed into geometrically simplified components i.e. U-shaped beams, also referred to as hat profiles or Omega (Ω) beams in the literature. The simplified geometries resemble components used in the automotive industry such as floor beams or pillar structures. However, the geometrical simplifications rationalizes evaluation and analysis of the geometrical distortions.

Two different dimensions of U-beams were produced, the first with a length x height x width of 1000 x 25 x 106 mm and the second with a length x height x width of 700 x 45 x 116 mm. The dimensional data of the U-beams are presented in Figure 10 and Table 3.

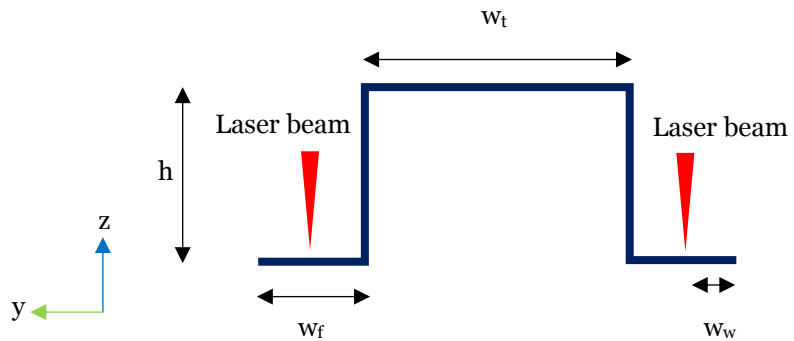


Figure 10 U-beam design

In addition to the U-beams, all materials were also made into flat sheets to fit the length and width of the U-beams. Thus, both single U-beam components (one U-beam combined with a flat sheet) and double U-beam components (two U-beams combined) were welded. The single and double

U-beam components, as seen in Figure 11 are asymmetrical and symmetrical, respectively, which exhibits different properties in terms of distortional behavior.

Table 3 U-beam dimensions

PAPER	Length	Height h	Flange width w_f	Top width w_t	Weld to edge w_w
B	1000	25	16	74	8
C-D	700	45	14	65	7

The two lower strength steel grades were cold formed into U-beam shapes. Due to the hot formed production of the UHSS material the 22MnB5 U-beams and flat sheets were hot formed.

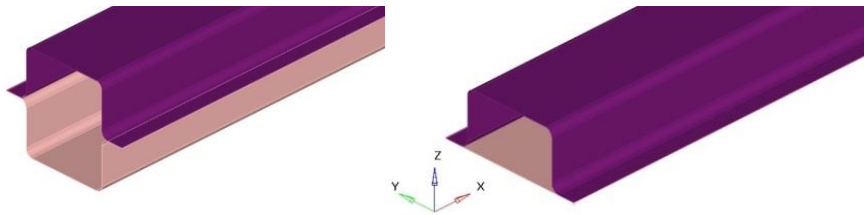


Figure 11 Symmetrical (left) and asymmetrical (right) U- beam components

The two components were welded in welding fixtures and support structures. The fixture and support structures were used to control the geometrical distortions and to simplify the measurements. In addition, the fixture was designed to resemble industrial applications in terms of the surrounding body in white structures. For the first components a vertical support structure with six supports, which hindered downward displacement at every 200 mm was used, as illustrated in Figure 12. Moreover, a toggle clamp was placed at the end of the U-beam, which applied a vertical force at the end. Thus, the beam was free to move upwards vertically at one end and free to move horizontally along the beam.

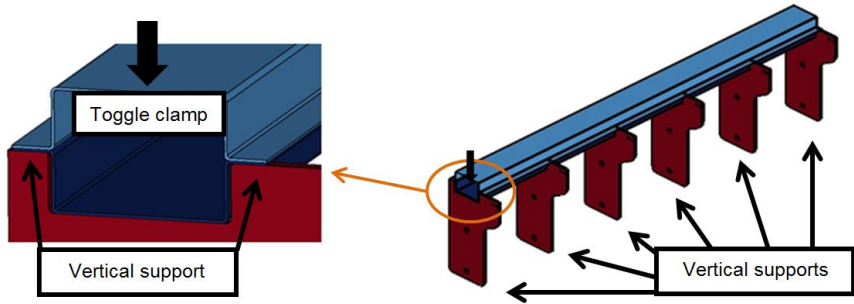


Figure 12 Support structure for first components

For the second components a pneumatic support structure, as shown in Figure 13, was used. The five clamping pairs provided vertical supports of 40 mm in width each as well as a downward pressure of 4 bar. Thus, during welding the component was hindered to move both vertically and horizontally during welding. However, after unclamping the structure was free to move horizontally and upwards vertically along the entire beam. After welding the clamping was released pair by pair; the first pair (H5 and V5) were released 180 seconds after welding and the pairs 2, 3 and 4 were released after another 10 seconds for each clamping pair. Finally, pair 1 was released after another 30 seconds.

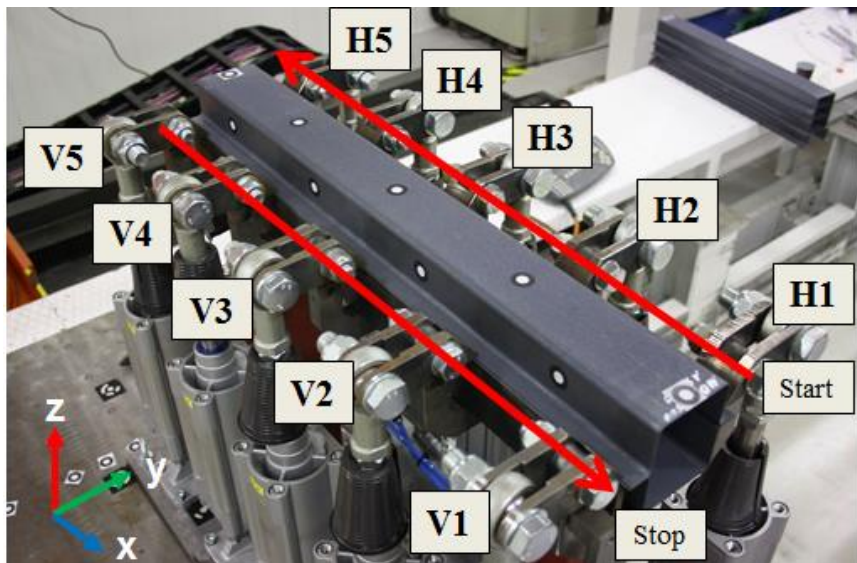


Figure 13 Support structure for second components

3.4 Welding equipment and process parameters

All of the LBW was performed in a semi-industrial laboratory environment using a Nd:Yag laser source, model name Trumpf HL4006D. The laser spot had a diameter of 0.6 mm and was focused on the top surface of the top metal sheet. A compressed air gas flow of 25 l/min was directed at the laser focus point during the welding. During the experimental regime different heat inputs per unit length were used in order to investigate the effect of heat input on the magnitude and distribution of the geometrical distortions. The welding velocity, welding power and heat input per unit length are presented in Table 4.

Table 4 Process parameters of experimental welding

PAPER	Nominal welding power [W]	Welding velocity [mm/s]	Heat input per unit length [J/mm]
B	4000	80	50
	2400	80	30
	4000	40	100
C-D	4000	25	160
	4000	58.3	69
	4000	125	32

All welds were located along the flanges of the U-beam close the longer edge as indicated by the red arrows in Figure 10. The total weld length was 980 mm for the 1000 mm long beams and 690 mm for the 700 mm long beams.

3.5 Experimental result evaluation and analysis

In order to measure the geometrical distortions in a relevant and accurate manner, a control measuring method was controlled as described below. All measurements were performed using a digital caliper.

For the first components, used in Paper B, the beams transverse dimensions were measured before and after welding in order to gain the transverse distortions due to welding. The longitudinal bending was measured by distance between the support and the beam at the center of the unclamped end.

For the second components, used in Paper C and D, the measurements were done after the unclamping regime after the welding outside the

support structure. All beams were measured before and after welding for the transverse distortions. The longitudinal bending was measured in a separate fixture with a toggle clamp at one end and measured at the other. The measuring principles are illustrated in Figure 14.

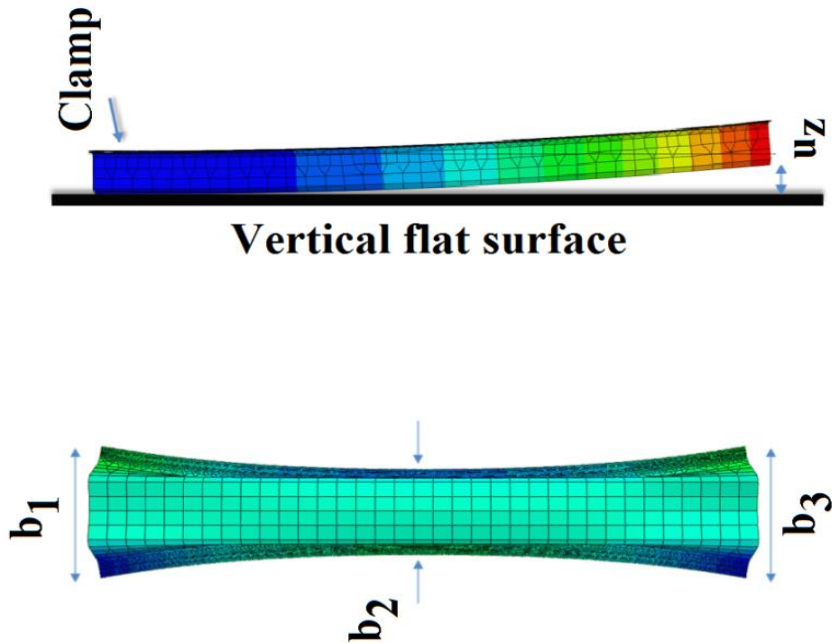


Figure 14 Measurements for the second components

In addition to the measurements of geometrical distortions all welds were inspected in terms of weld quality. The inspections included measurements of weld penetration depth, burn through of sheets, spatter, porosity, etc. These characteristics of the weld result are important to gain understanding of the heat transfer mechanisms during welding in order to model the welding accurately.

3.6 Numerical modeling of laser beam welding

The present thesis will investigate numerical modelling of the experimental welding described above by FE models. In order to develop complete numerical models of the LBW process several aspects of the physical phenomena must be modelled numerically. Also, as mentioned earlier, the present study aims to simplify and make the numerical models

more time efficient to implement into industrial environments. The modelling principles and possible methods for simplification are described below.

A typical FE approach to model geometrical distortions due to LBW involves both a thermal and a mechanical module. The thermal module describes the heat generation due to the laser source and the heat losses due to the boundary conditions of the system through conduction, convection and radiation. The thermal module will compute temperatures in the system. The mechanical module will translate the temperatures into mechanical strains and deformations with regard to the mechanical boundary conditions.

The interaction between the thermal and mechanical module - or coupling, may be done in several methods. The most detailed coupling is to translate the temperatures into mechanical deformations in every time step. One simplification used in the present study is to compute all time steps in the thermal module and then compute all time steps of the mechanical module. One further simplification is to reduce the transient behaviour of the mechanical module to compute all deformations in one step. This one-step method is often called the shrinkage method as it only models the shrinkage during the cooling after welding. The shrinkage method can be done by reducing the temperature in one computation step from an elevated temperature to the ambient temperature instantly. The one-step method has been investigated in the present thesis with different methods to generate the elevated temperature field.

To compute the thermal and mechanical modules both thermal and mechanical material models are required. Due to the temperature cycle during the LBW process and the alterations in material properties during heating and cooling of the steel materials extensive material models are required to capture the full material behaviour of the materials in the study. However, the material testing to acquire full material models is often costly and time consuming and requires specialist competence and equipment often not found outside research facilities. Thus, the present research will investigate the possibilities of simplifying material models, for example by only using material data at ambient temperature, to save pre-processing as well as computation times.

The computations were performed on two computation clusters, one with Intel Xeon E7-4850 and one with 16 core Intel Itanium 1.6 GHz processors.

4 Results and discussion

This chapter includes all the results the thesis as well as discussions regarding the implications of the results. The chapter is divided into three sub chapters. Firstly, a digital joining process planning approach is presented as an alternative to the traditional physical process planning. Secondly, the results of the experimental joining is presented. The results include distribution and magnitude of geometrical distortions due to LBW and present significant factors which influence distortions. Thirdly, modeling details of several numerical models for prediction of geometrical distortions due to LBW are presented as well as the results from the models. The models' agreement with the experiments and the computation times are presented and discussed.

4.1 Digital process planning of joining

The process planning of joining was analyzed by value stream mapping (VSM) in order to identify activities, actors and times of the process planning. The VSM depicts the different phases of the product development process including process planning. The VSM was also used to analyze the work flow in order to identify appropriate ways to incorporate digital tools in the process planning. The result of the VSM and the proposed additions of digital tools are illustrated in Figure 15 below.

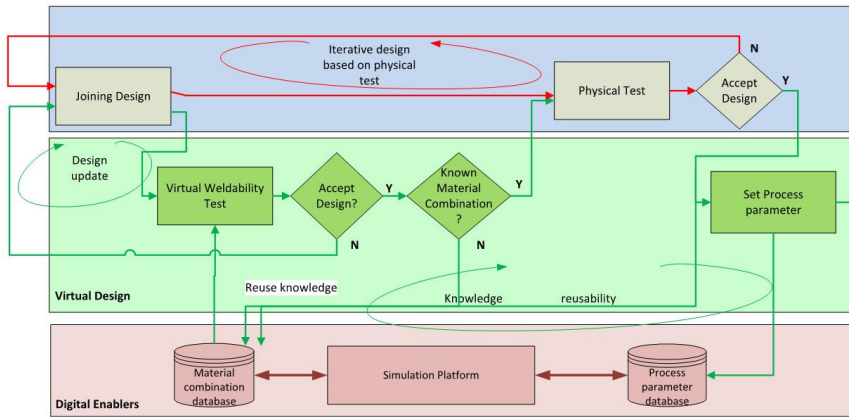


Figure 15 Design iterations of physically based process planning (blue) and digital process planning with digital tools (green and red) [45]

In Figure 15 the traditional physical process planning is illustrated by the blue rectangle where only physical tests are used to evaluate a process design and decide if it can be accepted or not. The VSM identified two digital tools which can be used to digitalize the process planning. The two tools – digital weldability tests and improved data handling by databases are illustrated in the green and red rectangles in Figure 15. The two digital tools are described below from both a technical and a practical perspective.

The goal of the RSW process planning is to define a set of process parameters, which can guarantee robust welding in an industrial environment with sufficient weld size and without spatter. This definition of process parameters can be reached by two methods. Firstly, it can be reached by assessment of weldability of a material combination and secondly it can be reached by re-use previous knowledge. Both these methods have been improved with two separate digital tools as will be described below.

A digital tool, based on FEM, to assess the weldability of a certain material combination was implemented in the digital process planning approach. FEM models can be used determine the main goal of the RSW process planning; to determine a successful set of process parameters which meet the criteria of sufficient weld size and avoid weld spatter. The FEM models have been developed and refined during the past decades to model the RSW process more accurately [46]. The development and refined and also efficiency have included more detailed mechanical, thermal and electrical

material models and constitutive models of the materials. The models have also been updated with new coupling or un-coupling of the mechanical, thermal and electrical modules in order to achieve both accuracy and time efficiency of the modeling. The outcome of the FEM model can be used to interpret both weld size and occurrence of spatter during the weld cycle of given set of process parameters. A typical screenshot comparing a physical cross section of a spot weld compared to an equivalent simulation is shown in Figure 16.

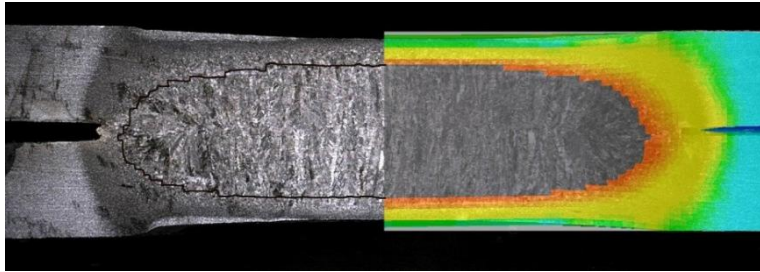



Figure 16 Metallographic section cut of physical weld (left) and simulation (right)

A database with a digital interface which can re-use knowledge from previous weldability assessments, both physical and digital, was implemented in the process planning. As many industrial actors have a long experience of weldability trials and the re-use of knowledge was seen to not be optimized – many identical weldability trials were repeated – a digital tool for knowledge re-use was developed. The tool also incorporates tolerances for sheet coating type and sheet thickness to re-use knowledge. By finding assessment of similar material combinations, the process planning can still reach its goal of determining the feasibility of process parameters. The tool was developed as a Microsoft Excel interface, as seen in Figure 17, to increase accessibility for all actors in the joining process planning.

2T 3T 4T			
	Material	Coating	Thickness [mm]
Sheet 1	DP600	GI50/50	1.8
Sheet 2	DP800	GI50/50	1.0
Sheet 3			
Sheet 4			

Electrode	B16
-----------	-----

SEARCH



RESULTS				
	JPS	Electrode	Minimum pitch	Weldability
Match:	21-2320	B16	25mm	OK
Similar:	21-2818	B20	30mm	OK

Figure 17 Screenshots of database search interface (above) and results regarding weldability (below) [47]

To measure the influence of the digital tools, the effect of the digital process planning approach on lead times for a body in white application was estimated. As a case study, a body in white pillar structure was selected. The results of the estimation are presented in Table 5.

The estimation of the physical process planning is based on discussions with experienced design and manufacturing engineering from VCC's body in white departments. When using a physical process planning approach a large part of the lead time is composed of time spent on purchasing and ordering and delivery times of the physical test specimens. This lead time may be repeated for several material types in each iteration as the Table shows.

The estimation of the digital process planning is based on computation times of RSW FEM simulations [46]. Typical computation times are in the duration of approximately 1 hour for a single weld and using full digital

utilization, simulations can run interrupted during the process planning stage. They are also less dependent of working hours or personal and can thus run around the clock.

In the final iteration it is recommended, as a precautionary measure, to perform verifying experimental test of the process parameters. As seen in Table 5, the potential lead time reduction is significant from a total of 20 weeks to total of 9 weeks based on a typical iterative re-design process involving three iterations. The estimation highlights the potential of digital tools to reduce process planning lead times in body in white applications.

Table 5 Estimated comparative assessment of physical and digital process planning

Body in white development stage	Physical process planning	Digital process planning
First proposal	5 weeks	2 weeks
Iteration 1	5 weeks	1 weeks
Iteration 2	5 weeks	1 weeks
Final product	5 weeks	5 weeks
Sum	20 weeks	9 weeks

4.2 Geometrical distortions due to laser beam welding

From the experimental methods described in Chapter 3, measurements of geometrical distortions due to LBW were assessed. From the variations in the experiments a range of influencing parameters on the distribution and magnitude of geometrical distortions were identified. The significant factors that were identified are structure geometry, sheet thickness, heat input and material grade. These factors are treated in separate sections below.

4.2.1 Influence of structure geometry on geometrical distortions

Four different structure geometries were studied in the present thesis. Two symmetrical, or double U-beam geometries of lengths of 700 mm and 1000 mm and two asymmetrical, or single U-beam geometries of the same lengths.

It was seen that the symmetrical and asymmetrical geometries exhibited distinctively different distortional behavior due to welding as illustrated in Figure 18. The symmetrical structures' geometrical distortion was

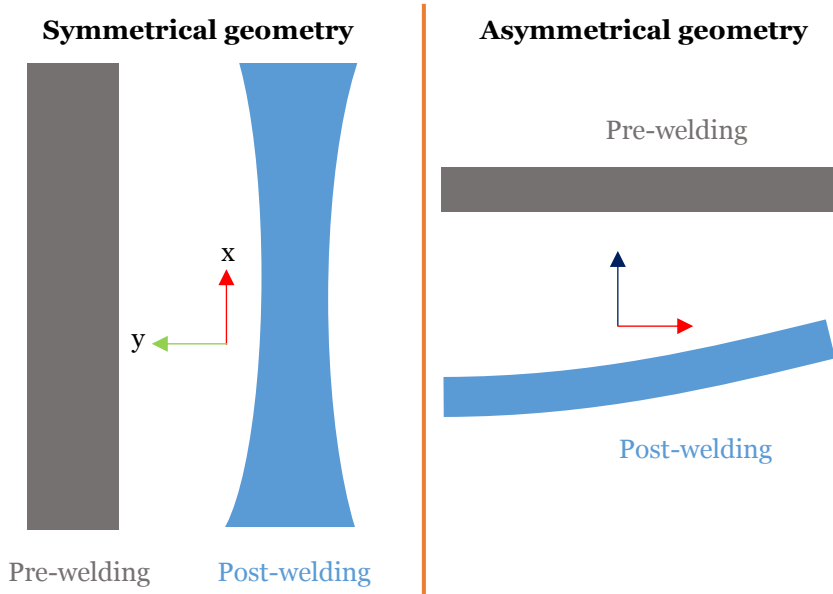


Figure 18 Dominant distortion modes of symmetrical structures (left) and asymmetrical structure (right) due to welding

dominated by transverse distortions, i.e. widening and narrowing of the beam, while the other distortion modes were negligible. Meanwhile, the asymmetrical structures exhibited significant longitudinal bending, i.e. vertical movement of the beam end, while the transverse distortions were negligible.

The distinctively different distortion modes of the two structures can be explained by the stiffness of the individual components of the structures and the imposed stresses from the welding.

The transverse distortion and longitudinal bending are controlled by in-plane stiffness and the bending stiffness, respectively. The in-plane stiffness of the flat sheet is very high compared to the U-beam. Conversely, the longitudinal bending stiffness of the flat sheet is very high compared to the U-beam. Consequently, the asymmetrical geometry is prone to bending and highly restrained to transverse distortions while the symmetrical geometry is restrained to bending and prone to transverse distortions.

The heating and cooling during the LBW process imposes expansive and contractive forces and stresses in the structure. The forces act in all

directions from the weld both transverse to and along the welding direction. Thus, the stresses also act in all directions. The stresses transverse to the welding direction will impose a transverse shrinkage in the structure. Moreover, the moving heat source will create a temperature gradient along the welding line which imposes stresses and forces along the weld length. If the welding line is out of the neutral plane of the structure, as in the asymmetrical structure, a lever arm is created resulting in a longitudinal bending moment.

Thus, both the stiffness of the components and the distance between the welding line and the neutral plane of the structure add to the effect of the transverse distortions of the symmetrical beam and the longitudinal bending of the asymmetrical beam. The magnitude of the distortions are presented in more detail in the following sections.

4.2.2 Influence of sheet thickness on geometrical distortions

In the asymmetrical 1000 mm long structure, different sheet thickness configurations were welded. Sheet thickness is an important parameter for body in white applications as it significantly affects both structural strength and crashworthiness as well as weight, which are both highly important product properties. The reference configuration included a flat sheet with a thickness of 1.0 mm and a U-beam with a thickness of 1.0 mm. Configurations where the flat sheet, the U-beam or both were increased to a thickness of 1.5 mm were welded. Thus, in total four thickness configurations were welded.

The results of the four configurations are presented in Figure 19. Linking to the reasoning in the previous section, the magnitude of the longitudinal bending is dependent on both the longitudinal bending stiffness of the components and the longitudinal bending moment which is a function of the distance between the neutral plane and the welding line.

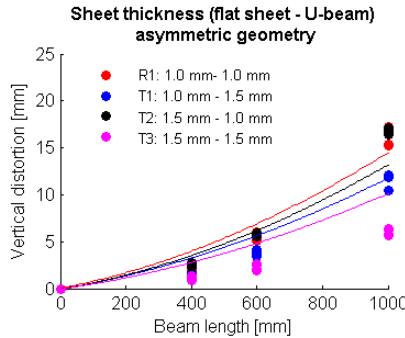


Figure 19 Longitudinal bending distortions in varying sheet thickness configurations

The bending stiffness is increased with the thickness of the sheet for both the flat sheet and the U-beam. Consequently, the thinnest configuration exhibits the largest distortions. However, increasing the sheet thickness also affects the lever arm between the faying surface where the weld is located and the axial forces are imposed and the neutral plane of the structure. In the configuration where the flat sheet is 1.5 mm and the U-beam is 1.0 mm, the bending stiffness is increased but the lever arm is also increased, causing a larger bending moment. Consequently, the two effects counteract each other and the total change in final distortion is only 0.6 mm compared to the reference case.

In the other two configurations, where both components are 1.5 mm and when the flat sheet is 1.0 mm and the U-beam is 1.5 mm, the two factors – longitudinal bending stiffness and longitudinal bending moment - are cohering and the geometrical distortions are consequently reduced compared to the reference case.

4.2.3 Effect of heat input on geometrical distortions

The total heat input of the LBW process is expected to affect both weld quality and global geometrical distortions. As more heat is applied to the structure, higher and more widespread thermal strains are induced in the material expected to result in larger deformations. The additional heat by higher laser beam power may also increase weld penetration or, if excessive, impose weld faults into the material.

In the present study, the total heat input was varied in two different ways; firstly, by altering process parameters such as welding velocity and laser beam power and secondly, by welding intermittently, i.e. where the welding was applied as shorter stitches along the weld line.

The intermittent welding was employed in the asymmetric and symmetric geometries of the 1000 mm long components. The results of the geometrical measurements are presented in Figure 20. As the figure shows, the welding with intermittent welding significantly reduces the geometrical distortions compared to the continuous weld pattern. By reducing the total weld length by 49.0%, the maximum distortions for the asymmetric and symmetric geometries were reduced by 48.4% and 52.9%, respectively. Thus, the total heat input and the magnitude of the maximum geometrical distortions indicate a near-linear relation.

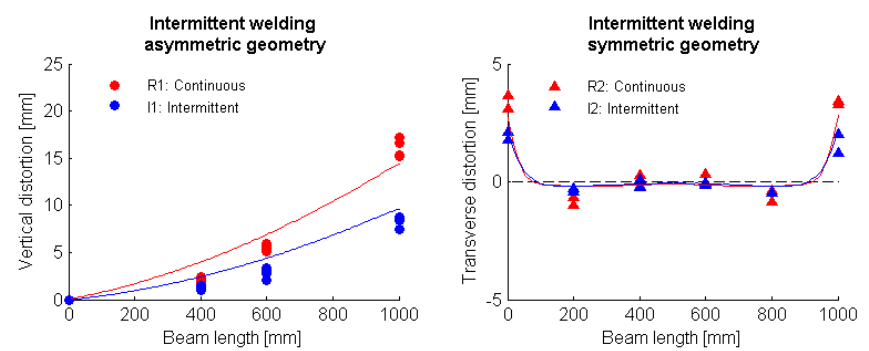


Figure 20 Influence of intermittent welding on asymmetric structure (left) and symmetric structure (right) of the 1000 mm beams

The variation of process parameters to vary heat input was employed in the asymmetric structure of the 700 mm beams and in both the asymmetric and symmetric structure of the 1000 mm beams. The results for the 1000 mm structures and the 700 mm structures are presented in Figure 20 and Figure 21, respectively.

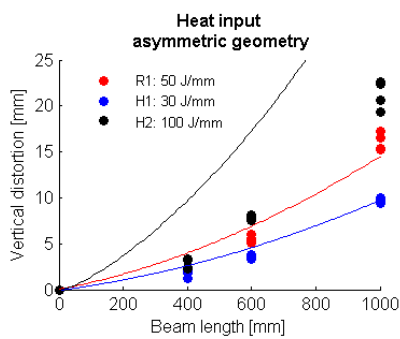


Figure 21 Influence of heat input on asymmetric structure of the 1000 mm beams

In the 1000 mm beams, the heat input was varied from 50 J/mm to 100 J/mm and 30 J/mm. When decreasing the heat input by 40 %, the maximum distortions was decreased by 40 %. However, when increasing the heat input by 100 %, the maximum distortion was increased by 32 %. During the higher heat input welding, significant welding faults were seen through intermittent burn-through and cutting along the weld line. The results indicate that not all welding power resulted in additional thermal strains in the material resulting in geometrical distortions.

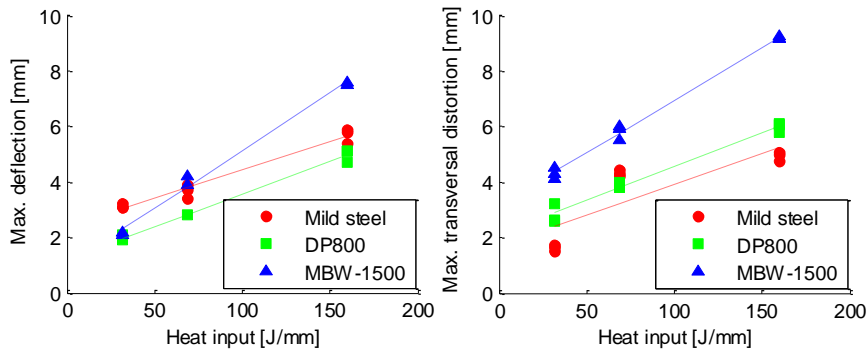


Figure 22 Influence of heat input on asymmetric structure (left) and symmetric structure (right) of the 700 mm beams

In the 700 mm beam, the heat input varied from 69 J/mm to 32 J/mm and 160 J/mm for both cross sections. In the 700 mm beam the relation between heat input and maximum geometrical distortion is showing a near linear relation for each cross section and material grade. However, as in the 1000 mm structure, the highest heat input level of 160 J/mm resulted in significant burn through and cutting along the weld line.

In both structure lengths the lower heat input level resulted in partial penetration welds. The partial penetration mode results in an additional bending moment was more thermal strains are introduced in the top sheet compared to the bottom sheet. This additional bending moment will reduce the effect of heat input on the maximum geometrical distortion for the asymmetric cross section where longitudinal bending is dominant.

4.2.4 Influence of structure material on geometrical distortions

The material grade of the structure's influence on geometrical distortions is of interest to investigate due to the trend in industry towards higher strength materials to increase the strength to weight ratio of the structure. For the 700 mm beams distortions were measured for materials with a nominal tensile strength of 200 MPa, 800 MPa and 1500 MPa. The higher

strength UHSS materials include alloying elements and heat treatments during production which may influence the geometrical behavior after welding. The distortion results of the different materials are presented in Figure 23.

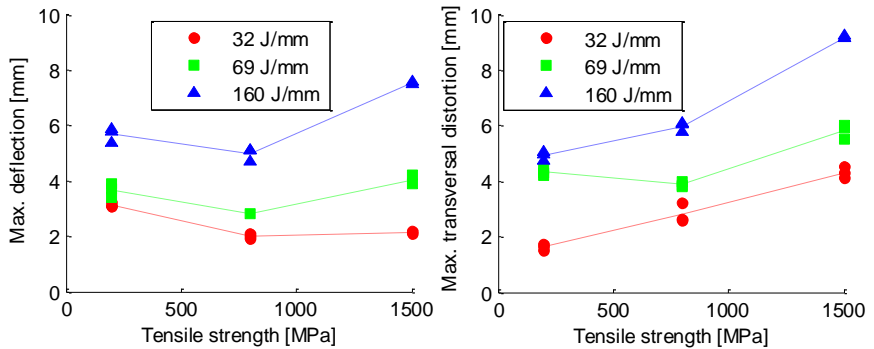


Figure 23 Influence of heat input on asymmetric structure (left) and symmetric structure (right) of the 700 mm beams

In both the asymmetric and symmetric structure the DP800 material exhibits the smallest distortions for all heat input levels. For the other materials, the mild steel and the UHSS 22MnB5 material, the geometrical distortions are of a higher magnitude. The results thus indicate a non-linear relation between tensile strength and magnitude of distortions.

A feasible explanation model to explain this non-linear relation is the relation between the magnitude of the plastic strains in the material and the size of the plasticized region. As the temperature rises near the weld zone during welding large thermal strains are imposed in the material. Due to the difference in yield limit between the materials, the weaker materials will experience a larger zone of plasticity as the material plasticizes at lower temperatures. However, the stresses which are due to the thermal plastic strains are of a higher magnitude in the higher strength materials. These higher stresses will add to the geometrical distortions of the high strength materials. This counter acting mechanisms when altering the yield limit of the material indicate the complex relation between material strength and magnitude of geometrical distortions.

At the same time, the yield limit is significantly reduced when the temperature is increasing. At very high temperatures – above the austenitization limit and close to the liquidus temperature the yield limit is similar between the materials. Consequently, in the higher strength materials, a larger amount of elastic strains and a smaller amount of plastic

strains are obtained. When the material subsequently cools, the elastic strains are relaxed and mainly the plastic strains contribute to the final distortions, except for remaining residual stresses.

4.3 Numerical modeling of geometrical distortions due to laser beam welding

As explained earlier, it is of interest to make process planning of joining process more efficient. For the LBW process a primary aspect of the process planning is the assessment and prediction of geometrical distortions due to LBW. While this assessment and prediction have traditionally been made with physical tests it may be replaced with numerical models. However, numerical models of welding processes may be extremely time consuming and unsuitable for industrial applications. Therefore, computational efficiency as well as accuracy of the models is a priority for industrial feasibility.

The following chapter present results and discussions from several different FEM based numerical models to predict distortions due to LBW. The models have used varying levels of modeling detail and simplification to reduce computational efficiency. The models are presented in terms of coupling procedure, thermal and mechanical modeling, predictive accuracy and computational and/or physical requirements and time efficiency.

4.3.1 Transient model

The so called transient model is the most detailed and complex numerical model of the LBW process used in the present thesis. The transient model, as the name suggests, solves the thermal and mechanical problem of the LBW process at numerous continuous time steps during the welding and cooling process. The solution of a previous time step is used as boundary conditions to the next. Thus, the continuous development of temperatures and distortions and a high level of detail and development over time is achieved in the results of the transient model. The transient model was evaluated for the mild steel, DP800 and 22MnB5 materials in both the symmetric and asymmetric 700 mm structures.

The transient model initially solves the thermal heat conduction problem in Equation 1 above. In the present thesis, a cylindrical Gaussian heat source moving along the weld line is used as the moving weld source. The conical Gaussian heat source was selected as it is assumed that complete weld penetration of the sheet stack-up is achieved during welding and

therefore less variations of heat supply in the thickness direction compared to partial penetration or conductive mode welding. In accordance with Equation 1 the beam efficiency was assumed to be 70%, h is the total thickness of the sheets (2 mm) and r_{beam} is the beam radius at the focus position (0.3 mm).

The thermal boundary conditions of the transient model are defined by the Stefan-Boltzmann law for radiation (using Stefan-Boltzmann constant, $\sigma = 5.67\text{e-}8 \text{ W m}^{-2} \text{ K}^{-4}$ and surface emissivity, $\varepsilon = 0.8$) and a thermal convection of $10 \text{ W K}^{-1} \text{ m}^{-2}$ to model heat losses at the sheet surfaces.

The thermal module generates a temperature field at numerous discrete time steps during the welding and cooling process. The thermal module uses the thermal material parameters density, heat conductivity and specific heat as presented in Figure 24 for all materials. As the Figure shows, the material data includes the effect of elevated temperature on the thermal material data. The density and specific heat data were obtained by the software THERMOCALC [48] computations and the conductivity was obtained by computations in the software IDS [49].

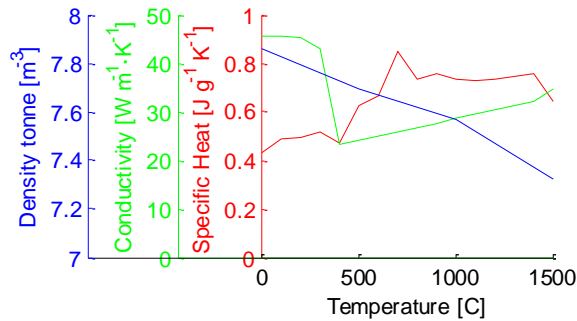


Figure 24 Thermal material parameters of the steel materials

The temperature field from the thermal solution is subsequently used as input to the mechanical module by imposing temperature gradients and resulting thermal strains in the model. The mechanical module is solved in a similar transient time step mode as the thermal module achieving results for geometrical distortions during the welding and cooling process. The mechanical module uses elastic and plastic material data as shown in Figure 25 Figure 26, respectively. In addition, a constant value of Poisson's ratio of 0.3 is used.

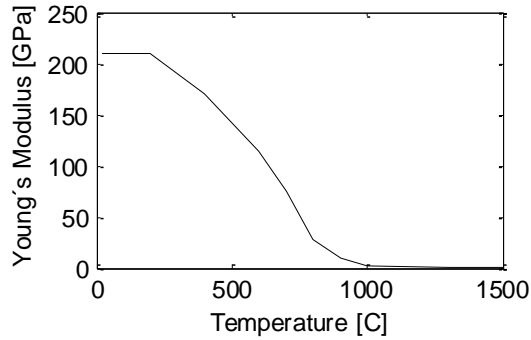


Figure 25 Young's modulus of the steel materials at elevated temperatures

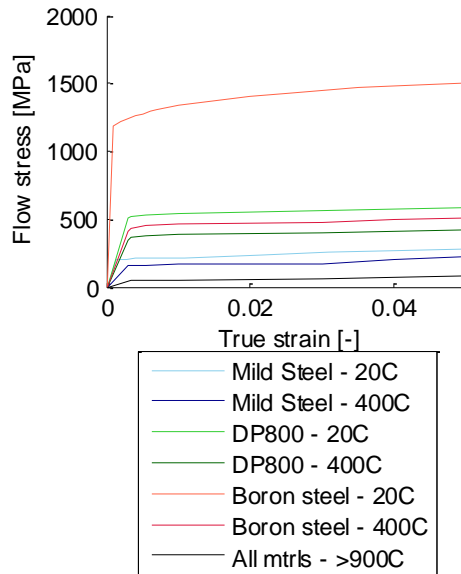


Figure 26 Plastic flow curves of steel materials at elevated temperatures

The geometrical distortions of the final time step are used for analysis and comparison to the experiments. The final maximum distortion of the asymmetric and symmetric structures are shown in Figure 27. The results from the transient numerical model shows a general good agreement with the experimental results. For both the asymmetric and symmetric

structure the model captures the influence of the heat input on the magnitude of the geometrical distortions.

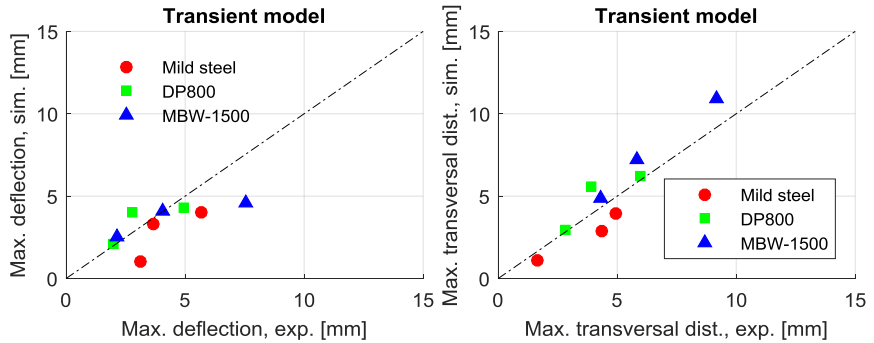


Figure 27 Geometrical distortion results of the transient model for the asymmetric structure (left) and the symmetric structure (right)

For the symmetric model the highest heat input of 160 J/mm the transient model tends to under-estimate the geometrical distortions for all materials. One source of the error is that the model does not include modeling of the non-continuous effects of the cutting mode and burn through which is achieved at excessive heat inputs.

The transient model is, due to its high level of detail and the numerous number of time steps, very time demanding. The models in the present study took in the order of approximately 2 to 3 days to be solved using a processor cluster of Intel Xeon E7- 4850 processors and the software ESI Sysweld as solver.

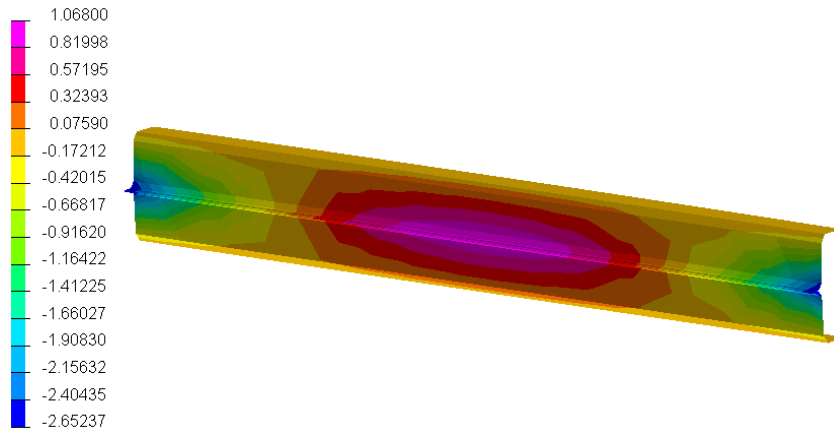


Figure 28 Transversal distortions of symmetrical geometry in transient model

4.3.2 Local-global model

Due to the long durations of the transient model it is of interest to industry to reduce computation times of the prediction of geometrical distortions due to LBW through numerical models to make joining process planning more efficient. Thus, the present research investigates different methods to simplify the modeling to reduce computations times and their influence on the accuracy of the models.

A new modeling approach, called the local-global model, was developed which uses simplified versions of both the thermal and mechanical module compared to the transient model. While the mechanical module is more time demanding than the thermal module, both modules take considerable time and time reductions would be beneficial to industry. The local-global model was evaluated for the mild steel, DP800 and 22MnB5 materials in both the symmetric and asymmetric 700 mm structures.

The results of the thermal module of the transient model shows that in LBW, high temperatures are only generated at the region very near the weld. Thus, the modeling of the surrounding global geometry has little influence on the temperature field of the region near the weld. Furthermore, the results show that the variations of temperature along the welding line is small except for the influence of the boundary conditions in the near proximity of the shorter ends. These observations is analogous with the use of smaller welding coupons to examine weld quality in physically based process planning.

From the observations above, a smaller – or local – model of 100 x 100 mm x 2 mm was developed for the thermal module. The local model was solved using the same heat source, material data and boundary conditions as used in the transient model as described in the previous section only with a smaller and simplified geometry. The solution of the local thermal model generates a transient temperature field along the condensed weld line. The maximum temperatures at a cross section are presented in Figure 29 showing increased temperatures with increased heat input. Solving the local thermal model takes in the order of 3 hours in FE solver ABAQUS using a 16 core Intel Itanium 1.6 GHz hardware setup.

The mechanical module has also been simplified compared to the transient model. As explained earlier, the dominant source of geometrical distortions due to welding are the shrinking distortions due to the cooling after welding. Thus, instead of modeling the transient temperature field during the welding and cooling during the LBW process, the temperature gradient can be induced into the mechanical model in one computation step. The temperature field from the local model is applied to the complete structure – or the global model of the structure. As no mechanical deformations occur at temperatures above the solidus temperature, the temperatures above the solidus temperature are not considered in the mechanical module as illustrated in Figure 29. The global mechanical model uses the same mechanical material data as the transient model but reduces the temperature in one single computation step to save computation time. The mechanical module is solved in the order of 15 minutes using the same setup as the thermal module.

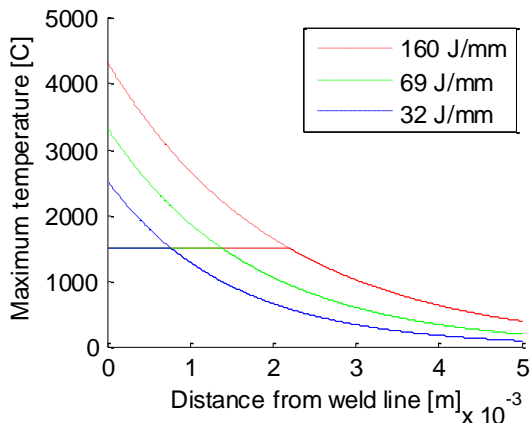


Figure 29 Maximum temperature profiles (dashed) and temperature field for global model (solid).

The results of the local-global model are presented in Figure 30. As the Figure shows the local-global shows general good agreement with the experimental results. Both the effect of heat input and material grade is captured with the model. However, the absolute error is somewhat greater than in the transient model.

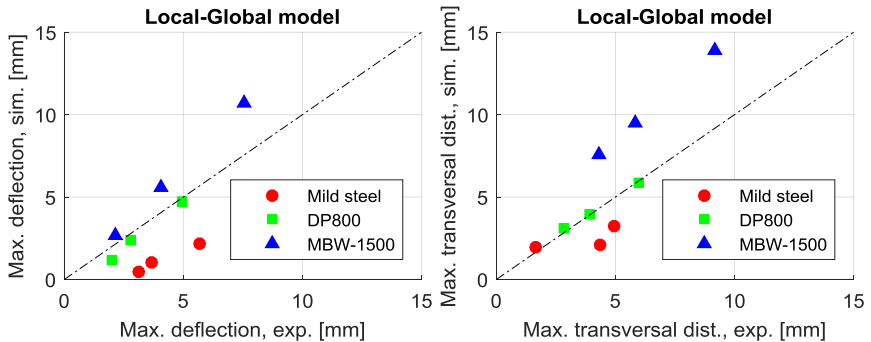


Figure 30 Figure 26 Geometrical distortion results of the local-global model for the asymmetric structure (left) and the symmetric structure (right)

In summary, the local-global uses underpinned assumptions of the LBW process and the mechanical behavior of the steel materials. These assumptions result in a simplified model with significantly reduced computation times and maintained predictive capabilities.

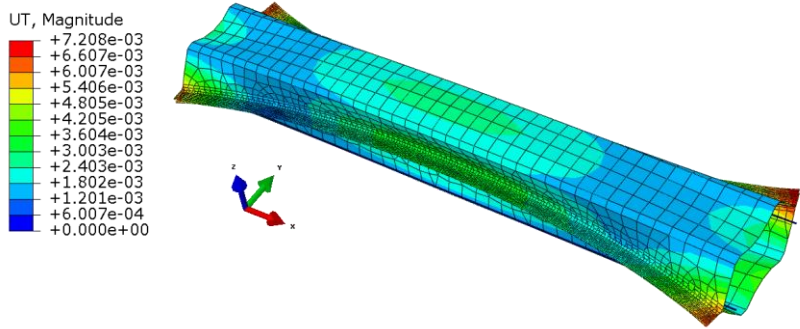


Figure 31 Transversal distortions of symmetrical geometry in the local-global model

4.3.3 Analytical shrinkage model

As discussed above, it is of interest to reduce computations times and modeling complexity to predict geometrical distortions due to the LBW process. As the local-global model shows, simplifications are possible depending on the required detail of the results.

A further simplification of both the thermal and mechanical model was developed by the so called shrinkage model. The shrinkage model replaces the continuous temperature field from the thermal module with a region of a constant elevated temperature close to the weld line. This region can be determined analytically as will be explained below and by a physically based calibration as will be explained in the next section. The analytically determined shrinkage model was evaluated for the VDA-239 CR-3 material and the 1000 mm structures.

By considering an idealized cross-section of the structure, Leggatt [50] presented a model for pure shrinkage of the cross section as in Equation 5 below.

$$\Delta w = (1 + \nu)\eta \frac{\alpha}{\rho c} \frac{q}{vt} \quad (5)$$

By applying the properties of steel at ambient temperature and the LBW process ($\nu = 0.3$, $\alpha = 1.2 \times 10^{-5} \text{ K}^{-1}$, $\rho = 7800 \text{ kg m}^{-3}$, $c = 460 \text{ J kg}^{-1} \text{ K}^{-1}$) and expressing the shrinkage as thermal strains, the size of the region of shrinkage can be expressed as in Equation 6. Details regarding the derivation of Equation 6 are further presented in PAPER B.

$$W = \frac{0.00348 \frac{q}{vt}}{\alpha \Delta T} \quad (6)$$

The shrinkage region, W , can be used as an equivalent solution to the thermal module to determine the temperature field during welding. As seen, the thermal module in the analytical is solved instantly and is not dependent of detailed temperature dependent material data or FEM pre-processing for obtaining the temperature field of the thermal model.

The mechanical module of the shrinkage model is solved in a similar way as in the global model of the local-global model in the previous section. However, the shrinkage region has a constant temperature gradient equal to the gradient between the solidus temperature and the ambient temperature. Also in order to reduce the complexity and material data prerequisites further only mechanical material data at ambient temperature was used. The results of the analytical shrinkage model are presented in Figure 32.

As Figure 32 shows the agreement between the numerical results from the analytical model and the experiments are generally good. The model generally captures the effect of structure geometry, sheet thickness, heat input and intermittent welding. However, the effect of excessive heat input when cutting and burn through is not captured as the model continuously grows as the heat input increases and the mechanical distortions are also increasing. Solving the mechanical modules takes in the order of 15 minutes using the FEM software ESI Weld Planner.

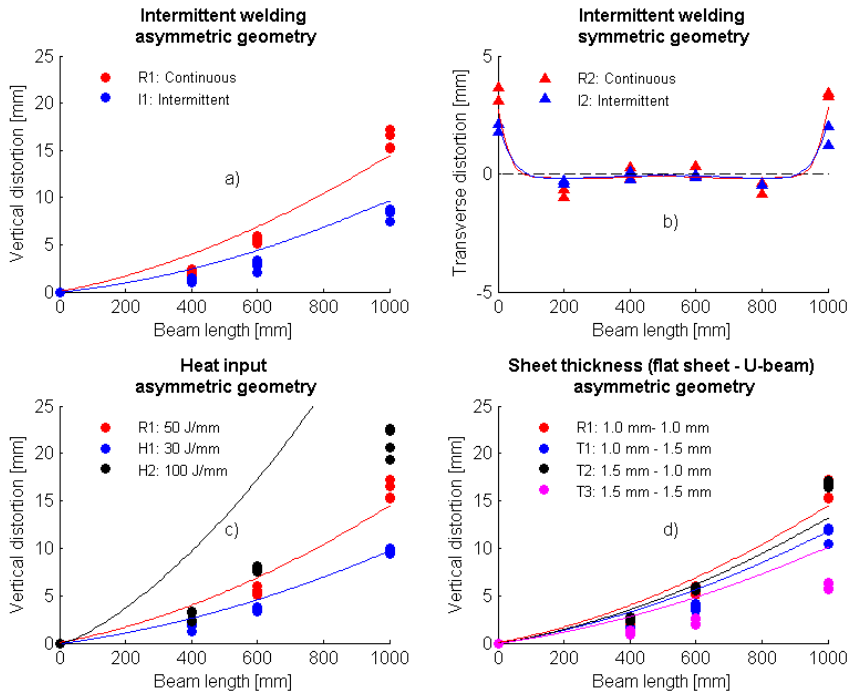


Figure 32 Geometrical distortion results of the analytical shrinkage model

4.3.4 Calibrated shrinkage model

The so called shrinkage model is based on the assumption that the dominant source to geometrical distortions due to LBW are the contractive thermal strains due to the cooling after welding. Thus, by replacing the transient temperature field which dynamically changes of time and along the welding line with a temperature field near the weld, the computation times can be significantly reduced. In the previous section a method to analytically determine the size of the temperature field was presented. However, in previous research it has been suggested to determine the size of the temperature field from a physical sample specimen. The width of the temperature field has been suggested to be twice the width of the molten zone of the weld as an approximation of the plasticized zone. The calibrated shrinkage model was evaluated for the mild steel, DP800 and 22MnB5 materials in both the symmetric and asymmetric 700 mm structures.

The determination of the temperature field was done by metallurgical section cuts. Several measurements were done along the weld and at different depths of the thickness. The measurements from the section cuts

were implemented into the global mechanical model to assess the geometrical distortions due to the LBW process. The results of the calibrated shrinkage model are presented in Figure 33.

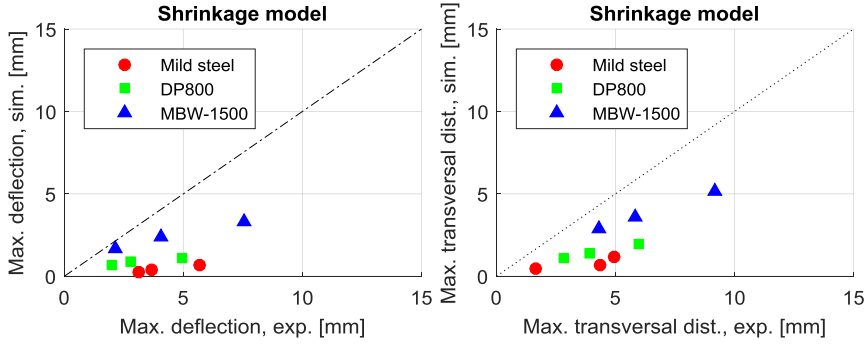


Figure 33 Geometrical distortion results of the calibrated shrinkage model for the asymmetric structure (left) and the symmetric structure (right)

The calibrated shrinkage model can capture the general distortion modes of the asymmetric and symmetric structures and their transverse distortions and longitudinal bending moment. As Figure 33 shows, the model can capture the general relation between the magnitude of the distortions and the total heat input. However, in all cases the model underestimates the magnitude of the distortions. Also, as in the other models the effect of material grade is captured with lower accuracy. The absolute error of the calibrated shrinkage model is somewhat greater than both the comparable transient model and the local-global model.

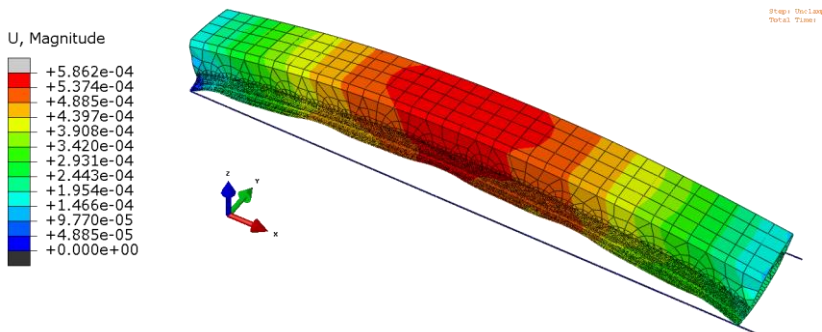


Figure 34 Vertical distortions of asymmetrical geometry in the calibrated shrinkage model

The calibrated shrinkage model requires physical welding of the sheet material and metallurgical section cuts of the specimens to ascertain the

size of the temperature field to be used in the global model. Thus, the total time requirement for the model is high and may be in the order of days or even weeks if the material or equipment is not available. Thus, the total time duration of the model is relatively long and can be in excess of the transient model.

5 Conclusions and future research

Process planning of joining was investigated and improved with a digitalized way of working. The digitalization was estimated to improve typical process planning time from approximately 20 weeks with a traditional physically based approach to approximately 9 weeks using the digital tools in a typical case with resistance spot welding for an industrial test case.

Geometrical distortions due to LBW were investigated by experimental trials and numerical models for prediction. The experimental investigation identified significant factors which influence the dominant distortion mode and the magnitude of the distortions. The investigation of numerical models assessed the accuracy and the efficiency of the numerical models depending on the model complexity. The absolute mean errors of the comparable FE models are presented in Figure 35.

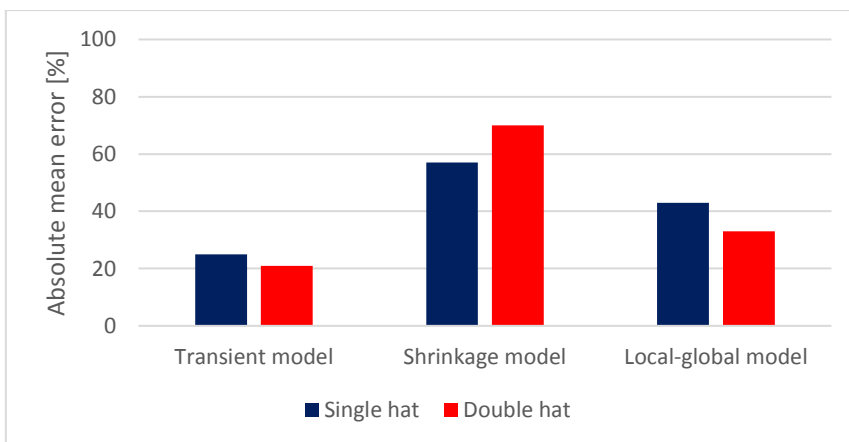


Figure 35 Absolute mean errors of FE models of 700 mm structures

This final chapter of the thesis will summarise the conclusions from this work as well as suggestions for future work.

5.1 Conclusions

In this thesis four research questions have been raised along with associated research hypotheses. The research questions and hypotheses focus on digitalization of process planning of joining and geometrical distortions due to LBW and numerical modeling of these geometrical distortions. The conclusions developed from the research hypotheses are as follows:

- The first hypothesis, which stated that “Digital engineering tools can be utilized to carry out process planning of joining processes” was confirmed from the results of the thesis. Digital tools in the form of numerical FEM models and databases were implemented in a process planning and an estimated reduction in process planning lead time of 11 weeks was estimated. The numerical FEM models were used for prediction of weld results which are faster than traditional physical testing. Moreover, a digital database was implemented which handled re-use of knowledge to improve process planning times and avoid redundant work effort.
- The second hypothesis, which stated that “Heat input, mechanical and thermal material parameters and global structural shape all affect the distribution and magnitude of geometrical distortions due to laser beam welding”, was confirmed from the results of the thesis. The experimental study investigated the influence of several parameters on the distribution and magnitude of distortions due to LBW. The results from the study identified several factors, including the ones in the hypotheses and their influence on the distribution and magnitude of distortions. The factors’ influence were presented and explained scientifically. The identification of the significant factors work as valuable guidelines for design and process engineers to find product and process solutions to avoid excessive geometrical distortions after LBW.
- The third hypothesis, which stated that “Numerical models can predict geometrical distortions with sufficient accuracy to be beneficial to process planning”, was confirmed. Several factors

which influence the distribution and magnitude of geometrical distortions due to LBW can be captured by the numerical models investigated in the thesis. While the accuracy varies with the different models, they all exhibit predictive accuracy which are beneficial in the process planning and product development.

- The fourth hypothesis, which stated that “Material models, heat transfer models, and numerical modeling can be simplified to become more efficient with maintained accuracy for engineering applications in industry” was confirmed. Three different numerical models were investigated in the thesis. All models included different levels of complexity or simplification of mechanical material modeling, thermal mechanical modeling and heat input modeling. The material models in the models included both material parameters at ambient temperature and the influence of elevated temperature on the material parameters. The heat transfer was modeled both using a phenomenological conical Gaussian moving heat source and an analytically determined temperature zone. By combining different levels of complexity in the different parts of the model depending on the allowed computation time a suitable modeling approach can be found. The computation times were reduced from up to 3 days to approximately 3 hours by introducing modeling simplifications.

5.2 Future research

The digital process planning approach presented in the thesis was evaluated for a smaller case study. In order to evaluate the impact of the digital process planning approach it would be of interest to evaluate the approach in a more comprehensive test case in a complete industrial application, for example a complete automotive body in white. The author suggests that the digital and traditional approaches should be compared simultaneously in parallel to determine the possible benefit of the digital tools.

Moreover, the numerical modelling of geometrical distortions due to LBW was performed on idealized and simplified geometries to measure distortions robustly. However, in industry, welding is performed on more complex continuous arbitrary geometries, which may affect distortional behavior of the components. Thus, it is of interest to evaluate the numerical

models in more complex geometries taken from industry, such as sub-assemblies, hang on parts or body in white applications.

Lastly, a recent major trend in the automotive industry is hybrid joining, where more than joining method is combined to realize beneficial product properties. For example, LBW is often combined with RSW and/or adhesive in industrial applications. To enhance the numerical models it is of interest to combine different joining methods in one model to predict geometrical distortions and joint properties.

References

- [1] S. Oberthür and H. E. Ott, The Kyoto protocol. Berlin [u.a.]: Springer, 1999.
- [2] J. Rogelj, M. Den Elzen, N. Höhne, T. Fransen, H. Fekete, H. Winkler, R. Schaeffer, F. Sha, K. Riahi, and M. Meinshausen, "Paris Agreement climate proposals need a boost to keep warming well below 2 °C," *Nature*, vol. 534, no. 7609, 2016.
- [3] P. Nieuwenhuis, A. Beresford, and A. K.-Y. Choi, "Shipping or local production? CO 2 impact of a strategic decision: An automotive industry case study," *Int. J. Prod. Econ.*, vol. 140, no. 1, 2012.
- [4] A. Topolansky, "Alternative fuels. Challenges and opportunities for the global automotive industry," *Columbia J. World Bus.*, vol. 28, no. 4, 1993.
- [5] R. H. Borcherts, H. L. Stadler, W. M. Brehob, and J. E. Auiler, "Improvements in automotive fuel economy," *Energy*, vol. 3, no. 4, 1978.
- [6] K. L. Edwards, "Strategic substitution of new materials for old: Applications in automotive product development," *Mater. Des.*, vol. 25, no. 6, 2004.
- [7] G. S. Cole and A. M. Sherman, "Light weight materials for automotive applications," *Mater. Charact.*, vol. 35, no. 1, 1995.
- [8] G. Meschut, V. Janzen, and T. Olfermann, "Innovative and highly productive joining technologies for multi-material lightweight car body structures," *J. Mater. Eng. Perform.*, vol. 23, no. 5, 2014.
- [9] Volvo Car Group, "Volvo XC90 body structure," Global Newsroom, 2017. [Online]. Available: https://www.media.volvocars.com/image/low/148215/1_1/5.
- [10] W. M. Steen and J. Mazumder, *Laser material processing: Fourth edition*. 2010.
- [11] H. Zhang and J. Senkara, *Resistance Welding: Fundamentals and Applications*. Taylor & Francis, 2005.
- [12] V. D. Bhise, *Automotive Product Development: A Systems Engineering Implementation*. CRC Press, 2017.
- [13] M. S. Shephard, M. W. Beall, R. M. O'Bara, and B. E. Webster, "Toward

- simulation-based design," *Finite Elem. Anal. Des.*, vol. 40, no. 12, 2004.
- [14] L.-E. Lindgren, "Numerical modelling of welding," *Comput. Methods Appl. Mech. Eng.*, vol. 195, no. 48–49, 2006.
 - [15] A. Einstein, "Strahlungs-Emission und-Absorption nach der Quantentheorie," *Verh. Dtsch. Phys. Ges.*, vol. 18, 1916.
 - [16] C. B. Hitz, J. Ewing, and J. Hecht, *Introduction to Laser Technology: Fourth Edition*. 2012.
 - [17] J. Ion, *Laser Processing of Engineering Materials*. 2005.
 - [18] J.-Y. Jeng, T.-F. Mau, and S.-M. Leu, "Prediction of laser butt joint welding parameters using back propagation and learning vector quantization networks," *J. Mater. Process. Technol.*, vol. 99, no. 1, 2000.
 - [19] M. Watanabe, K. Satoh, K. Kimura, and R. Hoshi, "Effect of Welding Methods and Sequences on the Residual Stress Distribution of Welded Joints," *J. JAPAN Weld. Soc.*, vol. 24, no. 4, 1955.
 - [20] M. Watanabe and K. Satoh, "Effect of welding conditions on the shrinkage distortion in welded structures," *Weld. J.*, vol. 40, no. 8, p. 377s–384s, 1961.
 - [21] C. Schwenk, T. Kannengiesser, and M. Rethmeier, "Restraint conditions and welding residual stresses in self-restrained cold cracking tests," in *ASM Proceedings of the International Conference: Trends in Welding Research*, 2009.
 - [22] T. Schenk, I. M. Richardson, M. Kraska, and S. Ohnimus, "A study on the influence of clamping on welding distortion," *Comput. Mater. Sci.*, vol. 45, no. 4, 2009.
 - [23] M. Seyyedean Choobi, M. Haghpanahi, and M. Sedighi, "Investigation of the effect of clamping on residual stresses and distortions in butt-welded plates," *Sci. Iran.*, vol. 17, no. 5 B, 2010.
 - [24] M. V. Deo and P. Michaleris, "Mitigation of welding induced buckling distortion using transient thermal tensioning," *Sci. Technol. Weld. Join.*, vol. 8, no. 1, 2003.
 - [25] P. Michaleris, "Modelling welding residual stress and distortion: Current and future research trends," *Sci. Technol. Weld. Join.*, vol. 16, no. 4, 2011.
 - [26] D. G. Richards, P. B. Prangnell, S. W. Williams, and P. J. Withers, "Global

- mechanical tensioning for the management of residual stresses in welds," *Mater. Sci. Eng. A*, vol. 489, no. 1–2, 2008.
- [27] Y. M. Omboko, S. Böhm, H. Verhoeven, P. Weigert, and H. Kurz, "Numerical Compensation Technique for determining Predeformation of weld distortions." 2012.
 - [28] D. Rosenthal, "The Theory of Moving Source of Heat and its Application to Metal Transfer," *ASME Trans.*, vol. 43, no. 11, pp. 849–866, 1946.
 - [29] D. T. Swift-Hook and A. E. F. Gick, "Penetration Welding with Lasers," *Weld. Res. Suppl.*, vol. 52, no. 11, pp. 492–499, 1973.
 - [30] W. M. Steen, J. Dowden, M. Davis, and P. Kapadia, "A point and line source model of laser keyhole welding," *J. Phys. D. Appl. Phys.*, vol. 21, no. 8, 1988.
 - [31] M. Lax, "Temperature rise induced by a laser beam," *J. Appl. Phys.*, vol. 48, no. 9, 1977.
 - [32] M. Lax, "Temperature rise induced by a laser beam II. the nonlinear case," *Appl. Phys. Lett.*, vol. 33, no. 8, 1978.
 - [33] J. Goldak, A. Chakravarti, and M. Bibby, "A new finite element model for welding heat sources," *Metall. Trans. B*, vol. 15, no. 2, pp. 299–305, 1984.
 - [34] S. A. Tsirkas, P. Papanikos, and T. Kermanidis, "Numerical simulation of the laser welding process in butt-joint specimens," *J. Mater. Process. Technol.*, vol. 134, no. 1, pp. 59–69, 2003.
 - [35] P. Lacki and K. Adamus, "Numerical simulation of the electron beam welding process," *Comput. Struct.*, vol. 89, no. 11–12, 2011.
 - [36] K. Kim, J. Lee, and H. Cho, "Analysis of pulsed Nd:YAG laser welding of AISI 304 steel," *J. Mech. Sci. Technol.*, vol. 24, no. 11, 2010.
 - [37] J. Kroos, U. Gratzke, and G. Simon, "Towards a self-consistent model of the keyhole in penetration laser beam welding," *J. Phys. D. Appl. Phys.*, vol. 26, no. 3, 1993.
 - [38] A. Kaplan, "A model of deep penetration laser welding based on calculation of the keyhole profile," *J. Phys. D. Appl. Phys.*, vol. 27, no. 9, 1994.
 - [39] K. N. Lankalapalli, J. F. Tu, and M. Gartner, "A model for estimating penetration depth of laser welding processes," *J. Phys. D. Appl. Phys.*, vol.

- 29, no. 7, 1996.
- [40] R. Fabbro and K. Chouf, "Keyhole modeling during laser welding," *J. Appl. Phys.*, vol. 87, no. 9, 2000.
 - [41] N. O. Okerblom, *The calculations of deformations of welded metal structures*. Her Majesty's Stationery Office, 1958.
 - [42] A. Bachorski, M. J. Painter, A. J. Smailes, and M. A. Wahab, "Finite-element prediction of distortion during gas metal arc welding using the shrinkage volume approach," *J. Mater. Process. Technol.*, vol. 92–93, pp. 405–409, 1999.
 - [43] G. Verhaeghe, *Predictive formulae for weld distortion - a critical review*. Woodhead, 1998.
 - [44] D. Tikhomirov, B. Rietman, K. Kose, and M. Makkink, "Computing Welding Distortion: Comparison of Different Industrially Applicable Methods," *Adv. Mater. Res.*, vol. 6–8, pp. 195–202, 2005.
 - [45] O. Andersson, D. Semere, A. Melander, M. Arvidsson, and B. Lindberg, "Digitalization of Process Planning of Spot Welding in Body-in-white," in *Procedia CIRP*, 2016, vol. 50.
 - [46] O. Andersson and A. Melander, "Prediction and verification of resistance spot welding results of ultra high strength steels through FE simulations," *Model. Numer. Simul. Mater. Sci.*, vol. 5, pp. 26–37, 2015.
 - [47] O. Andersson, "VCC RSW Toolbox Software." Volvo Car Group, 2017.
 - [48] B. Sundman, B. Jansson, and J. O. Andersson, "The Thermo-Calc databank system," *Calphad*, vol. 9, no. 2, pp. 153–190, 1985.
 - [49] J. Miettinen, S. Louhenkilpi, H. Kytönen, and J. Laine, "IDS: Thermodynamic-kinetic-empirical tool for modelling of solidification, microstructure and material properties," *Math. Comput. Simul.*, vol. 80, no. 7, pp. 1536–1550, 2010.
 - [50] R. H. Leggatt, "Distortion in welded steel plates," University of Cambridge, 1981.

Appendix A

Nominal alloying content of steel materials

	C	Si	Mn	P	S	Al	Nb	Ti	Cu	Cr+Mo	B
VDA-100 CR-3	0.08	0.5	0.5	0.025	0.02	0.01	-	0.3	0.2		
Mild steel	0.14	0.20	1.50	0.01	0.002	0.04	0.015	0.025	-	-	-
DP800	0.13	0.13	0.13	0.13	0.13	0.13	0.13	-	-	-	-
22MnB5	0.25	0.40	1.40	0.025	0.01	0.015	-	0.05	-	0.5	0.005